GENETIC AND BIOCHEMICAL ANALYSIS OF INNATE IMMUNITY IN *Arabidopsis thaliana*

A Dissertation

by

CHENG CHENG

Submitted to the Office of Graduate and Professional Studies of
Texas A&M University
in partial fulfillment of the requirements for the degree of

DOCTOR OF PHILOSOPHY

Chair of Committee,	Ping He
Co-Chair of Committee,	Libo Shan
Committee Members,	Timothy Devarenne
	Pingwei Li
Head of Department,	Gregory Reinhart

December 2013

Major Subject: Biochemistry

ABSTRACT

Perception of evolutionarily conserved pathogen-associated molecular patterns (PAMPs) elicits rapid and profound transcriptional reprogramming in hosts and activates defense to pathogen attack. The molecular signaling networks underlying this plant pattern-triggered immunity (PTI) remain fragmented. We identified a series of mutants with altered *pFRK1::LUC* activity were identified and named as *Arabidopsis* genes governing immune gene expression (*aggie*) through forward genetic screening. Map-based cloning identified *Aggie1* as encoding *Arabidopsis* C-terminal domain (CTD) phosphatase-like 3 (CPL3), a homolog of yeast FCP1 phosphatase that dephosphorylates the CTD of RNA polymerase II (RNAPII) during the transcription cycle. MAMP perception induced a rapid and transient CTD phosphorylation in *Arabidopsis*, underlying the modulation of CTD phosphorylation dynamics controlling plant immune responsive gene expression. Aggie1/CPL3 specifically dephosphorylated Ser2 of the CTD *in vivo* and *in vitro* and preferentially interacted with phosphorylated CTD. Transcriptional analysis indicates that *cpl3* showed overall enhanced flg22-mediated transcription responses. Thus, Aggie1 negatively regulates immune responsive gene expression essential for suppression of pathogen growth by modulating the phosphorylation status of RNAPII CTD. Cyclin-dependent kinases C (CDKC) functions as RNAPII kinases. Interestingly, we also found the silencing of *cdkc1* and *cdkc2* in wild type reduced flg22-mediated transcription responses and the plants were more susceptible to *Pseudomonas syringae* DC3000, suggesting their positive role in PAMP-triggered immunity.

Temperature fluctuation is a key determinant for microbial invasion into the host and for host evasion of the microbe. In contrast to mammals that maintain constant body temperature, plant internal temperature oscillates on a daily basis. It remains elusive how plants operate inducible defenses in response to temperature fluctuation. We report that ambient temperature changes lead to pronounced shifts of two distinct plant immune responses: pathogen-associated molecular pattern (PAMP)-triggered immunity (PTI) and effector-triggered immunity (ETI). Plants preferentially activate ETI signaling at relatively lower temperatures (10~23°C), whereas they switch to PTI signaling at moderately elevated temperatures (23~32°C). The *Arabidopsis arp6* and *hta9hta11* mutants, phenocopying plants grown at the elevated temperatures, exhibit enhanced PTI and yet reduced ETI responses. As the secretion of bacterial effectors favors low temperatures whereas bacteria multiply vigorously at elevated temperatures accompanied with increased MAMP production, our findings suggest that temperature oscillation might have driven dynamic co-evolution of distinct plant immune signaling responding to pathogen physiological changes.

DEDICATION

To my parents for their endless love and support, there is no chance that I could have done this without them.

ACKNOWLEDGEMENTS

I would like to thank my committee chair, Dr. Ping He and co-chair Dr. Libo Shan, for the great opportunity of my Ph.D. study in the exciting field of plant molecular pathology. I am extremely thankful for their generous support and their patient guidance for my PhD study.

Special thanks go to my committee members, Dr. Timothy Devarenne, and Dr. Pingwei Li, for their encouragement and advice. I also want to express my thanks to all my friends and colleagues in Ping and Libo's lab, in Department of Biochemistry and Biophysics, and in Department of Plant Pathology.

I would like to thank my parents for their endless support and all my friends for their encouragement throughout my doctoral program.

Finally, I would like to thank Shan Jiang for reading and making corrections to this dissertation.

NOMENCLATURE

AGGIE	*Arabidopsis* Genes Governing Immune Response
BAK1	Bri1-associated receptor kinase 1
BIK1	Botrytis-induced kinase1
CTD	Carboxyl-terminal domain
CDPK	Calcium-dependent Protein Kinase
CDKC	Cyclin-dependent kinase C
CERK	Chitin elicitor receptor kinase 1
CPL	CTD-phosphatase-like
DAMP	Damage-associated molecular pattern
DNA	Deoxyribonucleic acid
EDS1	Enhanced disease susceptibility 1
ERK	Extracellular signal-regulated kinases
ETI	Effector-triggered Immunity
E. coli	Escherichia coli
EF-TU	Elongation factor thermo unstable
EFR	EF-TU Receptor
FLS2	Flagellin-sensing 2
LRR	Leucine rich repeat
LPS	Lipopolysaccharide
MAb	Monoclonal antibody

MAPK	Mitogen-activated protein kinase
NDR1	Nonrace-specific disease resistance
NLR	Nucleotide-oligomerization-domain-like receptor
RNA	Ribonucleic acid
RNAPII	RNA polymerase II
RIN4	RPM1-interacting protein 4
RPS2	Resistance to *Pseudomonas syringae* 2
RPM1	Resistance to *Pseudomonas syringae pv. maculicola* 1
PAGE	Polyacrylamide gel electrophoresis
PAMP	Pathogen-associated molecular pattern
PCR	Polymerase chain reaction
PTI	PAMP-triggered Immunity
RNAi	Ribonucleic acid interference
RNase	Ribonuclease
RIPK1	RPM1-induced protein kinase 1
Ser	Serine
SDS	Sodium dodecyl sulfate
PEG	Polyethylene glycol
PRR	Pattern recognition receptor
T3SS	Type three secretion system
TIR	Toll/IL-1R
TLR	Toll-like Receptor

Tris	2-Amino-2-hydroxymethyl-1,3-propanediol
VIGS	Virus-induced-gene-silencing

TABLE OF CONTENTS

LIST OF FIGURES

LIST OF TABLES

CHAPTER I

INTRODUCTION AND LITERATURE REVIEW

The concept of plant immunity

The broad concept of plant immunity is the study of the organisms and of the environmental factors that cause disease in plants (Agrios, 2005). It is generally considered that two types of immunity exist in plant: pathogen associated molecular patterns (PAMPs)-triggered immunity (PTI) and Type Three Secretion system (TTSS) effector-triggered immunity (ETI). Although mammalian and plants have different defense systems, plenty of evidences suggest that these two types of the innate immunity are partial conserved between plants and animals (Nürnberger, Brunner, Kemmerling, & Piater, 2004; Stuart, Paquette, & Boyer, 2013). Both PTI and ETI play fundamental roles in innate immunity and are essential for host survival under different pathogen challenges. The innate immunity was discovered in mammalian systems in research led by Dr. Bruce A. Beutler and Dr. Jules A. Hoffmann, who won the Nobel Prize in Physiology or Medicine in 2011 (Lemaitre, Nicolas, Michaut, Reichhart, & Hoffmann, 1996; Poltorak et al., 1998). They discovered Toll-like receptors (TLRs) that recognize PAMPs and trigger downstream signaling pathways. However, the first plant PAMP receptor XA21 was discovered in rice in 1995, one year earlier than mammalian's TLR4's discovery. Besides PTI, another breakthrough in plant immunity field is the discovery of effector-triggered immunity (ETI). Different from PTI that causes a broad-spectrum disease resistance, ETI usually leads to a cultivar specific and more robust disease resistance. In

the early time, ETI also was named as gene-for-gene resistance. The first identified *Tomato* effector receptor Pto, which recognizes the *Pseudomonas syringae* effector protein avrPto, was identified by Gregory Martin in 1993 (Martin et al., 1993). The following year, another resistance gene RPS2 recognizing *Pseudomonas syringae* AvrRps2, was discovered by two independent groups (Bent et al., 1994; Mindrinos et al., 1994). This extraordinary research opened new doors to the largely unknown defense signaling pathways.

Pathogen-associated molecular patterns and their receptors

Pathogen associated molecular patterns (PAMP) are the molecules associated with groups of pathogens and are recognized by cells of the host innate immune system. In mammalian systems, the first identified PAMP and its corresponding receptor were lipopolysaccharide (LPS) and TLR4 (Poltorak et al., 1998), respectively. More PAMPs were identified later such as flagellin, recognized by TLR5, lipoteichoic acid, peptidoglycan, and nucleic acid variants normally associated with viruses, recognized by receptors TLR3 or unmethylated CpG motifs, recognized by TLR9. The first identified pattern recognition receptor (PRR) in plants is XA21 in rice in 1995, which provides strong resistance to the bacterium *Xanthomonas oryzae* pv. *oryzae* (*Xoo*), but the specific elicitor was identified 14 years later that turns out to be a 100% conserved Type I–Secreted peptide from *Xoo* (Lee et al., 2009; Song et al., 1995). In 2000, Thomas Boller's group identified the PRR FLS2 for flagellin from the bacterium *Pseudomonas syringae* (Gomez-Gomez & Boller, 2000). Later, their group identified the PRR EFR for bacterial elongation

factor Tu (EF-Tu) (Zipfel et al., 2006). The fungal chitin receptors CEBiP, and CERK1, LysM receptor-like kinases, were identified later in rice (Kaku et al., 2006; Miya et al., 2007). FLS2 and EFR, the Leucine-Rich Repeat Receptor Kinases (LRR-RKs), and Cerk1, the lysin motif receptor-like kinase (LysM-RLK), are all transmembrane receptors localized on the cytoplasmic membrane. The activation of these receptors by ligands results in the opening of calcium-associated plasma membrane anion channels and the release of negatively charged molecules (Jeworutzki et al., 2010).

Intracellular signal transduction in PTI

The exploration of PTI after receptor's discovery was followed by the identification of downstream signaling components: protein kinases such as BAK1, MAPK cascades; E3 ligases such as PUB12, PUB13, and transcription factors such as WRKY22, WRKY29 (Figure 1.1).

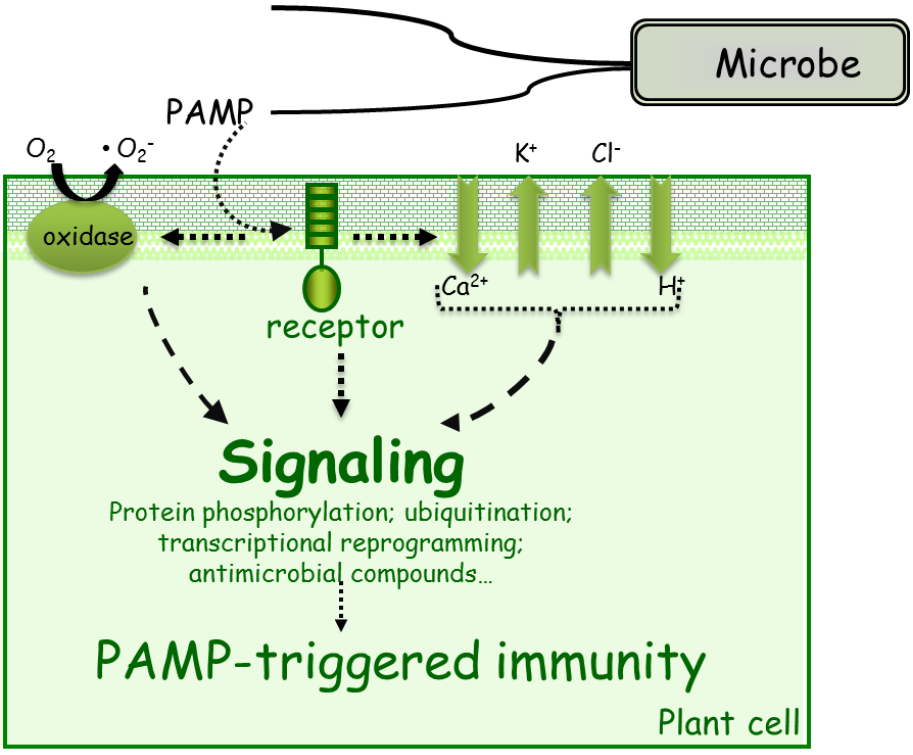

Figure 1.1 Model of PAMP-triggered immunity. Pathogen associated molecular pattern (PAMP), such as bacterial flagellin and EF-TU and fungal chitin can be perceived by the cell membrane receptors, and then transduce the signal through NADPH oxidase to produce superoxide (·O2–), and also through protein phosphorylation; ubiquitination to activate downstream signaling and transcriptional reprogramming; and finally produce antimicrobial compounds. This PAMP triggered immunity is called PTI.

BAK1

BRI1 associated kinase 1 (BAK1) functions as a co-receptor with brassinosteroid-insensitive1 (BRI1) and plays a positive regulatory role in brassinosteroid perception signaling. Later, Thomas Boller's group found that BAK1 was also associated with FLS2 and EFR, and plays a positive role in flg22 and elf18 mediated PTI pathway. The interplay of BAK1 between flg22 mediated and Brassinosteroid (BR) mediate signaling is

complicated: one research group concluded that BR inhibits PTI response in a BAK1 independent way, whereas the other group supported that BR modulates PTI in both BAK1-dependent and BAK1-independent manner (Albrecht et al., 2012; Belkhadir et al., 2012; Wang, 2012). BAK1 is a member of a five gene family and named as somatic embryogenesis receptor kinase (SERK). BAK1 is also known as SERK3. *bak1/serk4* double mutants showed seedling lethal phenotype, and BAK1 was then considered to be involving in cell death signaling (He et al., 2007). Recently, SERK1, 3, 4 were proven to be essential for BR perception signaling (Gou et al., 2012). BAK1 and SERK4 were shown to be essential for flg22 and elf18 mediated PTI responses (Roux et al., 2011).

MAPK cascade

The function of MAPK cascades on immunity was firstly extensively demonstrated in *Drosophila* and mammalians (Dong et al., 2002). Plant MAPKs are more closely related to the mammalian extracellular signal-regulated kinase (ERK) subfamily of MAPKs. The study of MAPK cascades in plant innate immunity has shown that MKK4/MKK5 is upstream of MPK3/MPK6 (Asai et al., 2002; Ichimura et al., 2006; Suarez-Rodriguez et al., 2007). MEKK1, MKK1/MKK2, and MPK4 were originally reported as negative regulator of plant immunity because the mutants of this cascade showed constitutive defense responses. However, recently it was shown that this constitutive defense responses might be caused by the activation of a R gene SUMM2 (Kong et al., 2012). Flg22 could trigger phosphorylation of MPK3, MPK6, and MPK4, MPK11(Bethke et al., 2012; Ranf et al., 2011). The second MAPK cascade involved in

the flg22-mediated PTI pathway is composed of MEKK1, MKK1/MKK2, and MPK4 (Ichimura et al., 2006; Suarez-Rodriguez et al., 2007; Veronese et al., 2006).

BIK1

BIK1 (Botrytis-induced kinase 1) was originally identified as a component in plant defense against necrotrophic fungal pathogens (Veronese et al., 2006). BIK1's transcriptional expression was strongly induced under Botrytis treatment and later was proven to play a positive role in flg22 and elf18 mediated PTI signaling pathways (Lu et al., 2010). BIK1, one of BAK1's substrate, interacts with both BAK1 and FLS2. BIK1 could also be phosphorylated by BAK1 under PAMP treatment. In turn, as a receptor-like cytoplasmic kinase, BIK1 could also phosphorylate FLS2 and BAK1. Researchers also found that BIK1 interacts with PEPR1 to mediate damage-associated molecular pattern peptide 1 (Pep1)-induced defenses in accordance with ethylene (Liu et al., 2013). Interestingly, the *Xanthomonas* effector AvrAC targets BIK1 by blocking its phosphorylation to attenuate plant defense (Feng et al., 2012).

Transcription factors

WRKY transcription factors are a large group TFs that play important roles in abiotic and biotic stress. WRKY transcription factors contain a WRKYGQK peptide sequence and a zinc finger motif (CX4–7CX22–23HXH/C), which generally binds to the DNA WRKY binding motif (Staskawicz et al., 1984). Earlier reports showed that WRKY22 and WRKY29 were induced upon flg22 treatment under MAPK cascades in

Arabidopsis, and played positive roles in innate immune responses (Asai et al., 2002). WRKY33 was first identified as strongly induced by pathogen infection, and then been shown as one of MPK3/MPK6's substrates, functions as a positive regulator on pathogen induced the camalexin biosynthesis pathway(Mao et al., 2011). Camalexin, an indolic secondary metabolite, is a major phytoalexin in Arabidopsis.

Effector-triggered-immunity

The concept of the plant pathogen effector originated from the 'gene-for-gene' concept raised by Flor in 1940s (Flor, 1942). The gene-for-gene theory was based on the observation that certain groups of plants were susceptible to one type of pathogen, whereas the other groups were not. Flor proposed that one for one relationship between an avirulence gene (Avr gene) in the pathogen and a resistance gene (R gene) in host (Flor, 1942). Specific avirulence proteins could be recognized by resistance proteins in host, and trigger defense responses and finally produce a resistant phenotype. The first two independent cases: the cloning of avr genes (a plethora of avr genes from *Pseudomonas syringae* pv. *glycinea* race 6) (Staskawicz et al., 1984) and the cloning of the resistance gene Pto from tomato (Martin et al., 1993) confirmed the gene-for-gene hypothesis. The cloning of RPM1, the R protein for *Pseudomonas syringae* type III effector AvrRpm1 and AvrB, reveals that Avr protein and resistance protein do not always interact directly; another interacting protein RPM1 Interacting protein 4 (RIN4) functions as a guardee to link Avr (effector) with R protein (guard) (Grant et al., 1995; Mackey et al., 2002). This model was proposed as the Guard Hypothesis (Bhattacharjee et al., 2011; Mackey et al.,

2002). RIN4 could be phosphorylated by AvrRpm1 or AvrB, and the phosphorylated RIN4 could activate RPM1 and trigger downstream defense response (Liu et al., 2011). Interestingly, another effector AvrRpt2 could cleave RIN4, and the elimination of RIN4 could activate resistance protein RPS2, and trigger downstream defense response (Axtell & Staskawicz, 2003; Mackey et al., 2003).

Resistance genes

Many of the resistance proteins are composed of Leucine-rich repeats (LRRs) and nucleotide-binding site (NBS) domains. However, some of the resistance proteins do not: for example, Pto is a serine/threonine kinase. The NBS-LRR class of R proteins is further sub-grouped: one group with a TIR domain (homology to the Drosophila Toll and mammalian Interleukin-1 receptors) at the N-terminus of the protein; the other group with a coiled-coil structure near the N-terminus. LRR domains are typically the key determinants for ligand receptor interaction (Axtell & Staskawicz, 2003; Liu et al., 2011). The rice resistance protein Pi-ta and its corresponding Avr protein from *Magnaporthe grisea* provide the direct evidence that LRR domain interact with Avr protein (Jia et al., 2000).

Dissertation overview

Our general interest is to investigate the molecular mechanism of plant innate immunity under bacterial pathogen infection. Chapter I is the introduction and background part of plant innate immunity. In chapter II, I focus on the genetic and biochemical

identification of *aggie1* mutants in plant innate immunity. In chapter III, I switch to temperature regulation of plant innate immune signaling.

Chapter II presents the identification and characterization of *Arabidopsis* genes governing immune gene expression 1(*aggie1*) in plant innate immune signaling. AGGIE1, also named CPL3, encodes a RNA polymerase II phosphatase. We found that pathogen associated molecular pattern, such as flg22, could enhance phosphorylation of RNA polymerase II. AGGIE1/CPL3 functions as a negative regulator for PAMP-triggered immunity, dephosphorylates RNA polymerase II to attenuate flg22 mediated transcriptional changes. Interestingly, we also found CDKC1 and CDKC2, function as RNA polymerase II kinases, and play positive role in plant innate immune signaling.

Chapter III presents the discovery of temperature regulated PAMP-triggered immunity and effector-triggered immunity. Ambient higher temperature could enhance PAMP-triggered immunity, and attenuate effector-triggered immunity. We also found that the non-canonical histone H2A.Z could functionally relate with temperature mediated immune responses. Two H2A.Z mutants: *hta9/11* and *arp6-10* phenotypically mimic higher temperature phenotype. Remarkably, those mutants showed enhanced PAMP triggered immunity and reduced effector-triggered immunity, indicating they are involved in temperature-mediated immune responses.

CHAPTER II

GENETIC DISSECTION OF PLANT INNATE IMMUNE SIGNALING NETWORKS

Summary

Perception of evolutionarily conserved pathogen-associated molecular patterns (PAMPs) elicits rapid and profound transcriptional reprogramming in hosts and activates defense against pathogen attack. The molecular signaling networks underlying plant pattern-triggered immunity (PTI) remain elusive. We have developed a sensitive genetic screen based on the early transcriptional changes upon MAMP perception in *Arabidopsis* transgenic plants carrying an early and specific immune responsive marker gene of the *FRK1* promoter fused with a luciferase (LUC) reporter. A series of mutants with altered *pFRK1::LUC* activity were identified and named as *Arabidopsis* genes governing immune gene expression (*aggie*). The *aggie1* mutants show elevated *pFRK1::LUC* induction upon multiple MAMP treatment or pathogen infection and enhanced resistance to virulent pathogen infection. Map-based cloning identified *Aggie1* encoding *Arabidopsis* C-terminal domain (CTD) phosphatase-like 3 (CPL3), a homolog of yeast FCP1 phosphatase that dephosphorylates the CTD of RNA polymerase II (RNAPII) during the transcription cycle. MAMP perception induced a rapid and transient CTD phosphorylation in *Arabidopsis*, underlying the modulation of CTD phosphorylation dynamics controlling plant immune responsive gene expression. Aggie1/CPL3 specifically dephosphorylated Ser2 of CTD *in vivo* and *in vitro* and preferentially interacted with phosphorylated CTD. Thus, Aggie1 negatively regulates immune responsive gene expression crucial for

restriction of pathogen growth by modulating the phosphorylation status of RNAPII CTD. Interestingly, we also found CTD kinase homologs, CDKC1 and CDKC2, in *Arabidopsis* and confirmed the kinase function on phosphorylating CTD Serine residues. We also detected reduced flg22 mediated gene induction and compromised disease resistance in the CDKC mutants. CPLs and CDKCs might work cooperatively on the phosphorylation status of RNAPII CTD to play a pivotal role in plant defense mediated transcriptional changes.

Introduction

Transcription of protein-coding genes in eukaryotes is intricately orchestrated by RNA polymerase II (RNAPII), general transcription factors, mediators and gene-specific transcription factors. The multi-subunit enzyme RNAPII is evolutionarily conserved from yeast to humans (Young, 1991). The largest subunit of RNAPII, Rpb1, contains a unique C-terminal domain (CTD) consisting of various repeats of a conserved heptapeptide with the consensus sequence $Y_1S_2P_3T_4S_5P_6S_7$ (Buratowski, 2009; Chapman, Heidemann, Hintermair, & Eick, 2008). The number of repeats varies from 26 in yeasts to 52 in mammals, and 42 in Arabidopsis. The vast combinatorial complexity of CTD posttranslational modifications constitutes a "CTD code" that is "read" by CTD binding proteins to regulate the transcription cycle, modify chromatin structure, and modulate RNA capping, splicing, and polyadenylation (Egloff & Murphy, 2008; Phatnani & Greenleaf, 2006). In particular, the CTD undergoes waves of serine phosphorylation and dephosphorylation events during transcription initiation, elongation and termination.

RNAPII is recruited to the pre-initiation complex (PIC) in an unphosphorylated state and rapidly phosphorylated at Ser5 residue by Cdk7 (cyclin-dependent kinase 7) in mammals (Esnault et al., 2008). During early elongation, Ser2 is phosphorylated by Cdk12 and Cdk9, whereas Ser5 phosphorylation level decreases (Bartkowiak et al., 2010; Qiu, Hu, & Hinnebusch, 2009). The phosphorylated CTD needs to be dephosphorylated by phosphatases for the next round of the transcription cycle to occur. During transcription elongation, Ser5 phosphorylation is removed by an atypical phosphatase Rtr1 (Mosley et al., 2009). Prior to termination, the remaining Ser5 phosphorylation is dephosphorylated by Ssu72 (Bataille et al., 2012). Fcp1 (TFIIF-associating CTD phosphatase) preferentially removes Ser2 phosphorylation. Fcp1, essential for yeast survival, is highly conserved among eukaryotes (Archambault et al., 1997; Kimura, Suzuki, & Ishihama, 2002). The conserved core of Fcp1 is composed of two essential modules: an FCP homology (FCPH) domain and a breast cancer 1 C terminus (BRCT) domain, both of which are required for phosphatase activity (Hausmann & Shuman, 2002, 2003). Structural and mutational analyses suggest that the FCPH domain belongs to the DxDxT superfamily of metal-dependent phosphotransferases (Ghosh, Shuman, & Lima, 2008; Kamenski, Heilmeier, Meinhart, & Cramer, 2004; Meinhart, Kamenski, Hoeppner, Baumli, & Cramer, 2005).

Little is known about the regulation of gene expression by CTD phosphorylation dynamics in plants. *Arabidopsis thaliana* contains a single *Rpb1* gene with a CTD of 42 heptapeptide repeats (Dietrich, Prenger, & Guilfoyle, 1990). Similar to human CDK7, *Arabidopsis* D type CDK (CDKDs) are major Ser5 kinases (Hajheidari, Farrona, Huettel, Koncz, & Koncz, 2012). The *Arabidopsis* genome encodes 20 CTD phosphatase–like

proteins (CPLs) categorized into three groups based on the structural similarity of protein domains (Koiwa et al., 2002; Koiwa, Bressan, & Hasegawa, 2006). CPL1 and CPL2 belong to group I CPLs containing a FCPH domain and one or two double-stranded RNA-binding motifs. CPL3 and CPL4 are group II CPLs with an FCPH domain and a BRCT domain. SSP (Scp1-like small phosphatase) proteins belong to group III CPLs with only FCPH domain. The CPL1 and CPL3, founding members of CPLs, were uncovered from a genetic screen for hyper-induction of the promoter for the plant abiotic stress response gene *RD29A* (Koiwa et al., 2002). Interestingly, the *cpl1* mutation renders the *RD29A* promoter hyper-active in response to cold, ABA, and salt treatments, whereas *cpl3* specifically mediates ABA response (Koiwa et al., 2002). Despite lacking the BRCT domain, group I and III CPLs could dephosphorylate Ser5 and/or Ser2 of *Arabidopsis* CTD (Feng et al., 2010; Jin et al., 2011; Koiwa et al., 2004; Ueda et al., 2008). However, it remains unknown whether CPL3 and CPL4, the prototype FCP phosphatases, are authentic CTD phosphatases and whether they possess any specificity towards CTD dephosphorylation. Moreover, how specific cellular responses regulate distinct CTD phosphorylation is poorly understood.

Map-based cloning identified *Aggie1* encoding *Arabidopsis* CPL3. Aggie1/CPL3 specifically dephosphorylated Ser2 of RNAPII CTD and preferentially interacted with phosphorylated CTD. Both FCPH and BRCT domains of CPL3 are required for its phosphatase activity and interaction with CTD. Importantly, *Arabidopsis* RNAPII CTD exhibited unique phosphorylation dynamics upon MAMP perception. Our study provides

a molecular link between general transcriptional regulation and specific immune responsive gene expression**.**

Material and methods

Plants growth conditions and bacterial inoculation

Arabidopsis wild-type (Col-0), *aggie1* and other plants were grown in Metro Mix 360 soil in a growth room at 23°C, 60% relative humidity and 75 μE m^{-2} s^{-1} light with a 12 hr photoperiod, 4 weeks old plants were used for protoplast isolation, bacterial inoculation or flg22 treatment.

Pseudomonas syringae pv. tomato DC3000 *(Pst)* or *Pseudomonas syringae pv. Maculicola (Psm)* strains were grown overnight at 28°C in the KB medium containing rifamycin or strepomycin (50 μg ml^{-1}). Bacteria were pelleted by centrifugation, washed, and diluted to the desired density. The leaves were hand-inoculated with bacteria using a needleless syringe, collected at the indicated time for bacterial counting, protein isolationor RNA extraction. To measure bacterial growth, two leaf discs were ground in 100 μl H_2O and serial dilutions were plated on TSA medium with appropriate antibiotics. Bacterial colony forming units (cfu) were counted 2 days after incubation at 28°C. Each data point is shown as triplicates. The statistical analysis was performed with SPSS software with one-way ANOVA analysis (SPSS Inc., Chicago).

RT-PCR and qRT-PCR

Total RNA was isolated from leaves or protoplasts with TRIzol Reagent

(Invitrogen). One μg of total RNA was used for complementary DNA (cDNA) synthesis with oligo (dT) primer and reverse transcriptase (New England BioLabs). qRT-PCR analysis was carried out using iTaq SYBR green Supermix (Bio-Rad) supplemented with ROX in an ABI GeneAmp® PCR System 9700. The expression of PTI and ETI marker genes was normalized to the expression of *UBQ10*. The regular RT-PCR was performed with 35 cycles. All the primers were listed in Table 1.

MAPK kinase activation, bik1 phosphorylation

To detect MAPK activity, 10-day-old WT, *aggie1* and *cpl3* seedlings grown on 1/2MS medium were transferred to water for overnight and then treated with 100 nM flg22 or H_2O for indicated time points and frozen in liquid nitrogen. The seedlings were homogenized in an extraction buffer containing 50 mM Tris-HCl, pH7.5, 100 mM NaCl, 15 mM EGTA, 10 mM $MgCl_2$, 1 mM NaF, 0.5 mM $NaVO_3$, 30 mM β-glycerophosphate, 0.1% IGEPAL, 0.5 mM PMSF, 1% protease inhibitor cocktail. Equal amount of total protein was electrophoresed on 10% SDS–PAGE. An α-pERK antibody (Cell Signaling) was used to detect phosphorylation status of MPK3 and MPK6 with an immunoblot.

For BIK1 phosphorylation assay, *Arabidopsis* protoplasts were transfected with HA epitope-tagged BIK1 and incubated at room temperature for overnight, pre-treated at 16, 23, or 28°C for 15 min and then treated with 100 nM flg22 or H_2O for 10 minutes. Total protein was separated by 10% SDS–PAGE gels followed by an α-HA immunoblot.

ROS production

ROS burst was determined by a luminol-based assay. At least 10 leaves of each four-week-old *Arabidopsis* plant were excised into leaf discs of 0.25 cm^2, following an overnight incubation in 96-well plate with 100 µl of H_2O to eliminate the wounding effect. H_2O was replaced by 100 µl of reaction solution containing 50 µM of luminol and 10 µg/ml of horseradish peroxidase (Sigma) supplemented with or without 100 nM of flg22. The measurement was conducted immediately after adding the solution with a luminometer (Perkin Elmer, 2030 Multilabel Reader, Victor X3), with a 1 min interval reading time for a period of 30 min. The measurement values for ROS production from 40 leaf discs per treatment were indicated as means of RLU (Relative Light Units). The experiments were repeated three times and similar results were obtained.

Map-based cloning

2.5 gram (approx. 125,000 seeds) of the FRK1-LUC seeds was treated with 0.4% EMS (ethane methyl sulfonate) for 8 hours. Approximately 7,000 M2 plants were screened for *aggie* mutants with the high or low luciferase activity under flg22 or hrcC treatment.

The F2 populations for mapping the aggie1 mutations were derived from genetic crossing between the mutants in the Col-0 background to wild-type plants in the *Ler* background. Bulked segregation analysis was performed on pools of 40 plants with INDEL markers between Col-0 and Ler. The primers used were listed in Table 1.

Protoplast transient assay

Protoplast isolation and transient expression assay were conducted as described (X. Gao et al., 2013; Dongping Lu et al., 2010). In general, 50 µl protoplasts at the density of 2 x 10^5 /ml and 10 µg DNA were used for promoter activity, 100 µl protoplasts and 20 µg DNA were used for protein expression and 500 µl protoplasts and 100 µg DNA were used for RT-PCR analyses.

RNA polymerase II phosphorylation in vivo

To detect phosphorylation status of RNAPII *in vivo*, 10-day-old WT, *aggie1* and *cpl3* seedlings grown on 1/2MS medium were transferred to water for overnight and then treated with 100 nM flg22 or H_2O for indicated time points and frozen in liquid nitrogen. The seedlings were homogenized in an extraction buffer containing 50 mM Tris-HCl, pH7.5, 100 mM NaCl, 15 mM EGTA, 10 mM $MgCl_2$, 1 mM NaF, 0.5 mM $NaVO_3$, 30 mM β-glycerophosphate, 0.1% IGEPAL, 0.5 mM PMSF, 1% protease inhibitor cocktail. Equal amount of total protein was electrophoresed on 10% SDS–PAGE. Monoclonal antibodies for detecting specific phosphorylated ser2, ser4, or ser7 were used detect phosphorylation status of RNAPII with an immunoblot.

RNA Sequencing analysis

Total RNA was isolated from seedlings with TRIzol Reagent (Invitrogen). Total RNA was purified using the RNeasy Mini Kit (Qiagen) following manufacturer's instructions and treated with RNase free DNase I (Qiagen) to remove genomic DNA. For

each timepoint, equal amounts of RNA from the two biological replicates were pooled for RNA-seq library construction.

RNA-seq library preparation and sequencing was carried out by Texas A&M AgriLife Genomics and Bioinformatics Service Lab (College Station, TX, USA). The libraries were sequenced on an Illumina HiSeq 2000 instrument with 100 bp single end (SE) reads. The total reads was around 15,000,000 per sample, corresponding 30X coverage for the whole transcriptome.

Identification of differentially expressed transcripts

The high-quality reads from each sample were mapped with the TAIR10 Gene Annotation reference assembly using CLC Genomics Workbench software. During alignment, at least 95% of the bases were required to align to the reference and a maximum of two mismatches were allowed. The total mapped reads number for each transcript was determined, and then normalized to detect RPKM (Reads per Kilobase of exon model per Million mapped reads). Fold changes were calculated based on the RPKM value by using Excel (Microsoft). Analysis was performed using the RNA-Seq module and the expression analysis module in CLC Genomics Workbench. Transcripts with relative fold change values of larger than 1.5 and RPKM value larger than 1 were included in analysis as differently expressed genes.

Virus induced gene silencing

PCR products used in the construction of silencing vectors were amplified from *Arabidopsis* cDNA using the VIGS primers. Primers were designed using Primer3 (Koressaar & Remm, 2007; Untergasser et al., 2012) and used to amplify a 400-bp fragment of CDKC1. The sequences were validated by PCR amplification of *Arabidopsis* cDNA followed by sequencing. Construction of VIGS vectors and *Agrobacterium*-mediated VIGS AtCDKC1 cDNA was amplified by PCR from Arabidopsis cDNA, and inserted into the pYL156 (pTRV-RNA2) vector by EcoRI and KpnI digestion. The primer sequences are 5'-CGGAATTCTGGACCCAGCCACAACTT -3' (CDKC1-F), 5'-GGGGTACCGGGAAAAGAAAGAGATTCAGTT-3' (CDKC1-R). Plasmids containing the binary TRV vectors pTRV-RNA1, pTRVRNA2 (pYL156) and pYL156 derivatives were transformed into *Agrobacterium tumefaciens* strain GV3101 by electroporation. *Agrobacterium* culture was grown for overnight at 28C in LB medium containing the antibiotics 50μg/ml kanamycin and 25μg/ml gentamicin, as well as 10 mM MES and 200 μM acetosyringone. The cells were pelleted by centrifugation at 1180 g at room temperature for 5 min, and re-suspended in infiltration culture containing 10 mM $MgCl_2$, 10 mM MES and 200 μM acetosyringone. Cell suspensions were incubated at room temperature for at least 3 h. Agrobacterium cultures containing pTRV-RNA1 and pTRV-RNA2 or its derivatives were mixed at a 1:1 ratio and infiltrated into two fully expanded cotyledons of 2-week-old plants using a needle-less syringe. VIGS experiments were repeated at least three times with more than six plants per repeat.

Protoplast transient expression of CPL3-GFP

C-terminal, N-terminal and full length GFP fusion of CPL3 were transfected into *Arabidopsis* protoplast cells. Protoplasts were observed 12 hour post transfection (hpt) with a confocal microscopy. Nuclear-localized RFP was co-transfected as nucleus-location control.

Table 1. Primers used in *aggie1* project

Mapping primers

Gene	Forward primer	Reverse primer
F4P9	TGGTCCATACCCATTTCATAAC	ATGAATTTTCATTCTACTGTTTTG
T1B8-2-F	CTTCAAAGCCTAGCTCAACAA	CGTCTTGCTCTGGTTCCTTC
ciw3	GGAAACTCAATGAAATCCACTT	GTGAACTTGTTGTGAGCTTTGA
F26B6	CTCTATCTGCCCACGAACAAG	GCCATTGCAAAAGAACATCAG
F16P2	CAGCAATCAAATAACGTGGTG	CTCTCTTCTTTCTTCGCCATTAG
F2H17	ATTGCATACCACGCAGTTCAC	CCATTTTGCCCTTTCCTTCTAC
AthBIO2b	TGACCTCCTCTTCCATGGAG	TTAACAGAAACCCAAAGCTTTC
F4P9-3	GATTGCTTTGATGAGCTCGA	ATTAGTCGTTAATATGTTGG
F4P9-4	CCTCCCTTGTAGGCTACCAT	CGTTGATACGTTTGGTTCG

Table 1. Continued

For CDKC1 VIGS construct

Gene	Forward primer	Reverse primer
CDKC1	TGTGGTATAGGCCCCCTGAA	GGGGTACCGGGAAAAGAAAGAGATTCAGTT

RT-PCR primers

Gene	Forward primer	Reverse primer
CDKC2	TGCCGATCAAAGTGTCTGAAG	GAGAATGTTGCTGCTGTGGA
UBQ10	AGATCCAGGACAAGGAAGGTATTC	AGATCCAGGACAAGGAAGGTATTC

qRT-PCR primers

Gene	Forward primer	Reverse primer
FRK1	ATCTTCGCTTGGAGCTTCTC	TGCAGCGCAAGGACTAGAG
WRKY30	GCAGCTTGAGAGCAAGAATG	AGCCAAATTTCCAAGAGGAT
At2g17740	TGCTCCATCTCTCTTTGTGC	ATGCGTTGCTGAAGAAGAGG
CPL3	CCAATTTACCTTGTCGGTTCC	AGCAGTTTGGTGCTGTCTGC
At1g07160	CGTGTTGGGGATTGATTCG	AGAGCTCGGGCGGTTATG
AT1G59865	AGTCGAGGCAAAGAAGGTTG	GCTTCACTTGTATCCACCAAGC
AT1G59860	CGCTGATTCCAAGCTTCTTC	GAAGACGATGACGGGAATTG
AT1G51920	CAAGAGCTCCTATTAGCTCGAGAAG	ATGGAGATTGAGAGTGGTGATGAG

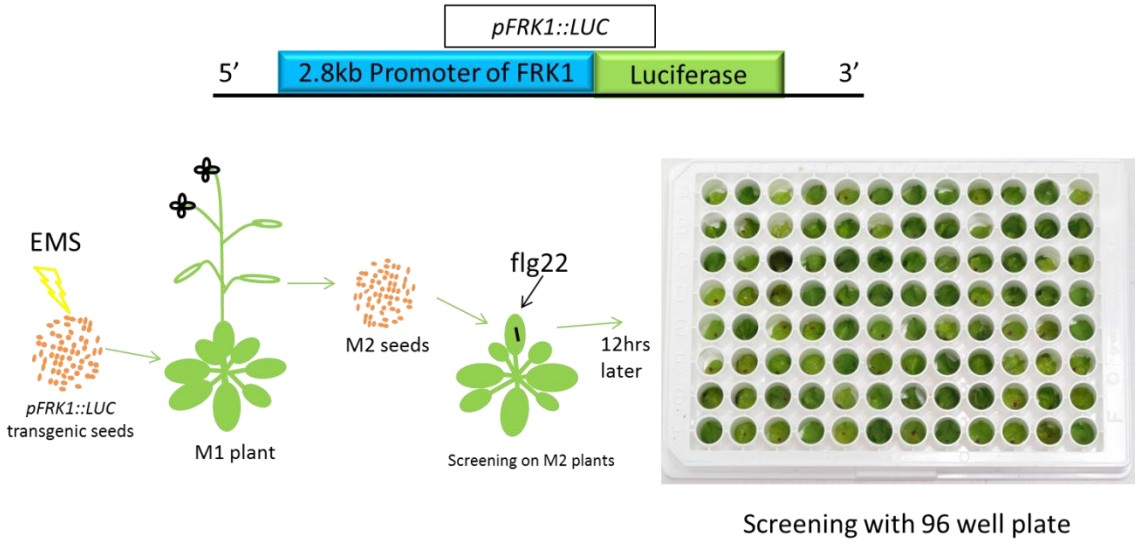

Figure 2.1 Schematic design steps for screening of *pFRK1::LUC* mutants.

Results

Forward genetic screening of pFRK1::LUC transgenic plants

To elucidate the signaling networks regulating immune gene activation, we developed a high throughput genetic screen with an ethyl methanesulfonate (EMS) mutagenized population of transgenic plants carrying *FRK1* promoter fused with a luciferase reporter gene (*pFRK1::LUC*) in *Arabidopsis* Col-0 plants. flg22 is a 22 amino acids bacterial flagellin peptide, it covers the core domain necessary for binding to its receptor FLS2 and biological activity in plant cells. *FRK1* (flg22-induced receptor-like kinase 1) represents a specific and early immune responsive gene activated by multiple MAMPs (Asai et al., 2002; He et al., 2006). The promoter of FRK1 was cloned and fused with luciferase gene and transformed into wild type *Arabidopsis* plants; and then the seeds

of transgenic plants were mutagenized by EMS. M1 plants were grown to get M2 seeds, and then the soil grown M2 plants were screened by infiltrated with flg22. 12 hours later after inoculation, the inoculated leaves were cut and put into 96-well plate; after spraying with luciferin, the substrate of luciferase enzyme, the plate was read in a luminometer to get a quantitative signal (Figure 2.1).

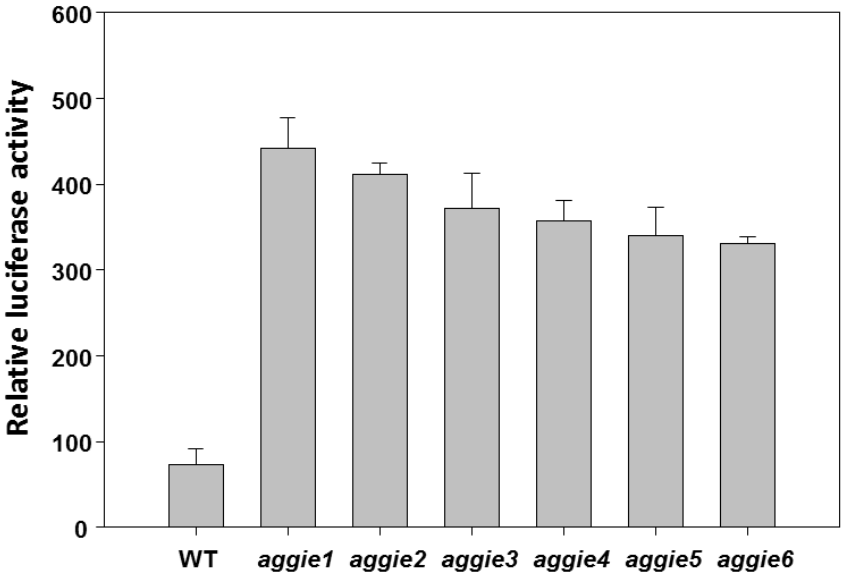

Figure 2.2 *aggie1 -6* mutants have enhanced *pFRK1::LUC* activity. First round of screening identified 6 *Arabidopsis*-Gene-Governing-Immune-Gene-Expression (*aggie)* mutants showing enhanced *pFRK1::LUC* activity under flg22 treatment.

Enhanced immune gene activation and disease resistance in aggie1 mutants

A series of mutants with altered *pFRK1::LUC* activity upon flg22 treatment were identified and named as *Arabidopsis* genes governing immune gene expression (*aggie*)

(Figure 2.2). The *aggie1* mutant, the one obtaining highest *pFRK1::LUC* activity under flg22 treatment, was further characterized and subjected for map-based cloning. Compared to WT plants, the *aggie1* mutants displayed elevated *FRK1* promoter activity upon flg22 treatment (Figure 2.3A, B). Notably, the *aggie1* mutants did not significantly activate *FRK1* promoter in the absence of flg22 (Figure 2.3A), suggesting specific regulation of *FRK1* expression by *Aggie1* in immune signaling. In addition to flg22, the *aggie1* mutants exhibited enhanced *pFRK1::LUC* activity in response to other MAMPs, including elf18, an 18-amino acid peptide of bacterial EF-Tu (Figure 2.3C). Similarly, the *pFRK1::LUC* activation by nonpathogenic bacteria *P. syringae* pv. *tomato* DC3000 *hrcC*, which is deficient in the delivery of type III virulence effectors, and non-adaptive bacteria *P. syringae* pv. *phaseolicola* NPS3121 was also enhanced in the *aggie1* mutants (Figure 2.3D). The activation of *FRK1* by these bacteria is likely attributed to collective action of a plethora of MAMPs. Apparently, the altered *FRK1* expression in the *aggie1* mutants was unlikely due to the mutation in specific MAMP receptors. Rather, the *aggie1* mutants may affect a downstream component in the convergent MAMP signaling. Consistent with the enhanced *FRK1* promoter induction, the *aggie1* mutants were more resistant to virulent *Pst* DC3000 infection. The bacterial population in the *aggie1* mutants was about ten-fold less than that in WT plants 4 days post infection (dpi) by dipping inoculation (Figure 2.3 E). The disease symptoms were also less pronounced in the *aggie1* mutant than that in WT plants (Figure 2.3F).

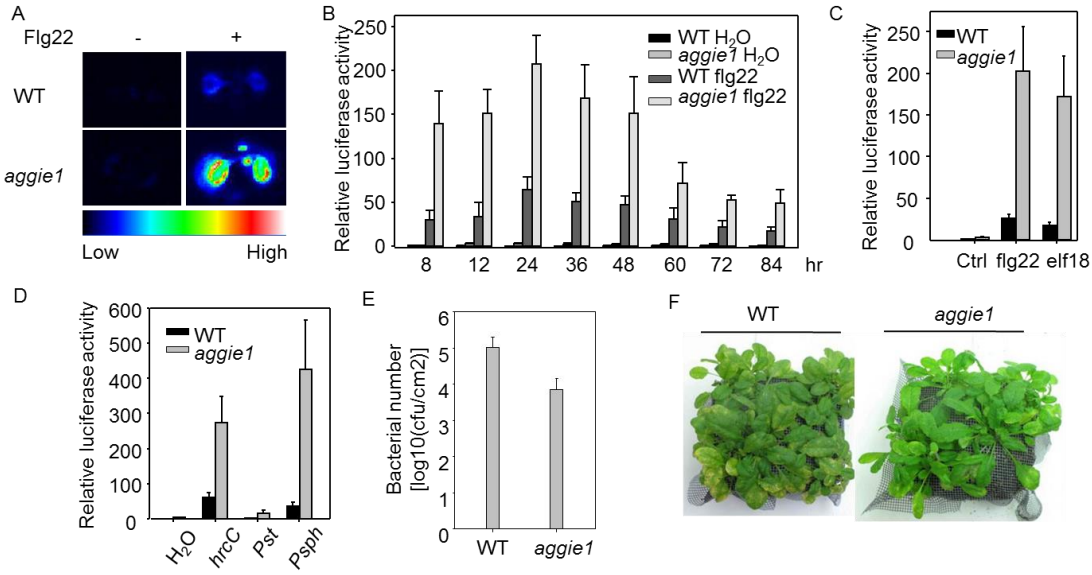

Figure 2.3 Elevated *pFRK1::LUC* expression and disease resistance in *aggie1* mutant. (A). Ten-day-old *aggie1* and wild-type (Col-0) seedlings were analyzed without treatment (control) and with 100nM flg22 treatment under CCD camara. (B). The *pFRK1::LUC* activity was enhanced in *aggie1* mutant upon flg22 treatment over 84 hrs. The WT (*pFRK1::LUC* transgenic) plants and *aggie1* mutants were hand-inoculated with 100nM flg22 and luciferase activity was measured at the indicated time points. (C) The *pFRK1::LUC* activity was enhanced in *aggie1* mutant upon different MAMP treatments. Plants were infiltrated with 100nM flg22 or 100nM elf18, and luciferase activity was measured 12 hr after infiltration. (D) The *pFRK1::LUC* activity was enhanced in *aggie1* mutant upon different pathogen infections. The plants were hand-inoculated with bacteria at 1 x 10^7 cfu/ml and the luciferase activity was measured 12 hr after inoculation. (E) The *aggie1* mutants are more resistant to *Pst* DC3000 infection. The plants were dipping inoculated with *Pst* DC3000 at 2 x 10^8 cfu/ml and bacterial growth assay were performed 3 days after inoculation. (F) Disease symptom of WT and *aggie1* mutants. The picture was taken 4 days after dipping inoculation.

Similarly, the *aggie1* mutants were more resistant to *Psm* infection with hand inoculation (Figure 2.4A). Besides bacterial elicitors flg22 and elf18, fungal chitin could trigger enhanced *pFRK1::LUC* activity in *aggie1* (Figure 2.4B).

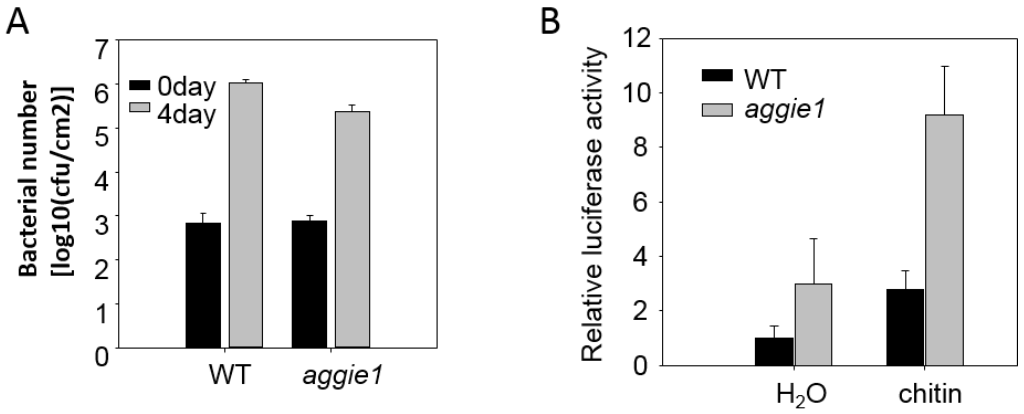

Figure 2.4 (A) Bacterial growth assay for aggie1 for *Pseudomonas syringae pv. Maculicola.* The *aggie1* mutants are more resistant to *Pseudomonas syringae pv. maculicola* infection. The plants were hand-inoculated with *Psm* at 1 x 10^4 cfu/ml and bacterial growth assay were performed 4 days after inoculation.(B) Enhanced *pFRK1::LUC* activities in *aggie1* under chitin treatment. The *pFRK1::LUC* activity was enhanced in *aggie1* mutant upon chitin treatments. Plants were infiltrated with 50ug/ml chitin, and luciferase activity was measured 12 hr after infiltration.

Unaltered MAPK activation, ROS production and Bik1 phosphorylation in the aggie1 mutants

MAPK activation and ROS production represent two early MAMP signaling events, which likely function upstream of *FRK1* expression. The flg22-induced MAPK activation detected by an α-pERK antibody in WT and *aggie1* seedlings suggested that *aggie1* did not affect flg22-induced MAPK activation (Figure 2.5A). Similarly, the *aggie1* mutants exhibited normal oxidative burst in response to flg22 treatment compared to WT plants (Figure 2.5B). These results suggest that Aggie1 functions either downstream or independently of MAPK activation and ROS production in MAMP signaling. Similarly,

Bik1 phosphorylation was comparable with wild type in *aggie1* mutant under flg22 treatment (Figure 2.5C).

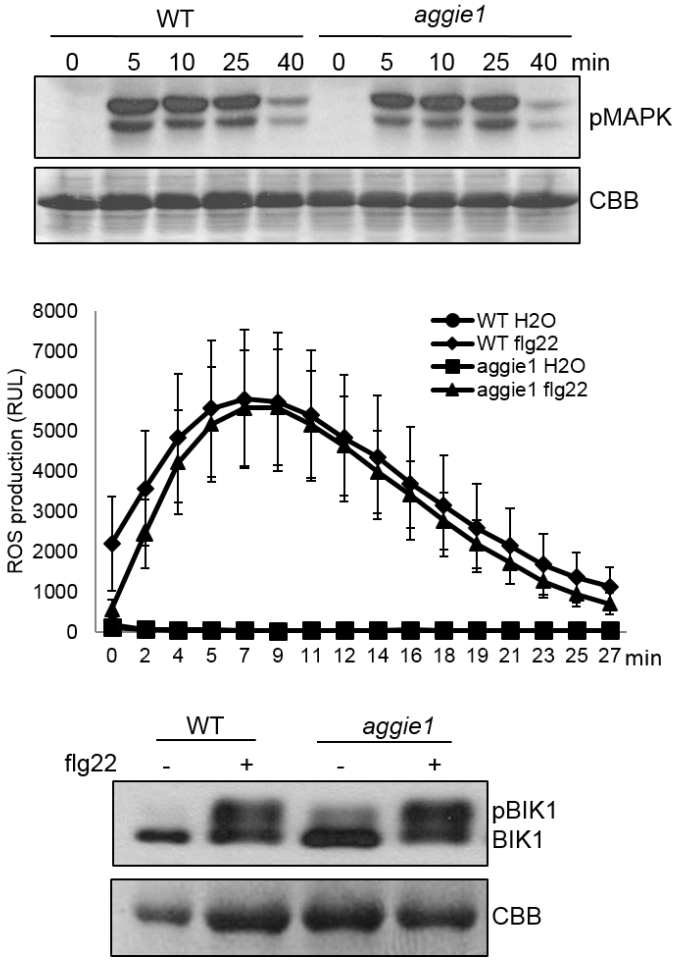

Figure 2.5 MAPK activation, ROS production and Bik1 phosphorylation in *aggie1* mutant. (A) Flg22-induced MAPK activation in wild type and mutants. Twelve-day old WT or *aggie1* seedlings were treated with 100nM flg22 for different time points. MAPK activation was analyzed with an anti-pERK antibody (top panel), and the protein loading was shown by Coomassie blue staining (CBS) (bottom panel). (B) flg22-induced ROS burst in wild type and mutants. Leaf discs were treated with H_2O (Ctrl) or 100 nM flg22. The data are shown as means ± standard errors from 40 leaf discs. (C) flg22-induced Bik1 phosphorylation in protoplast of wild type and mutants.

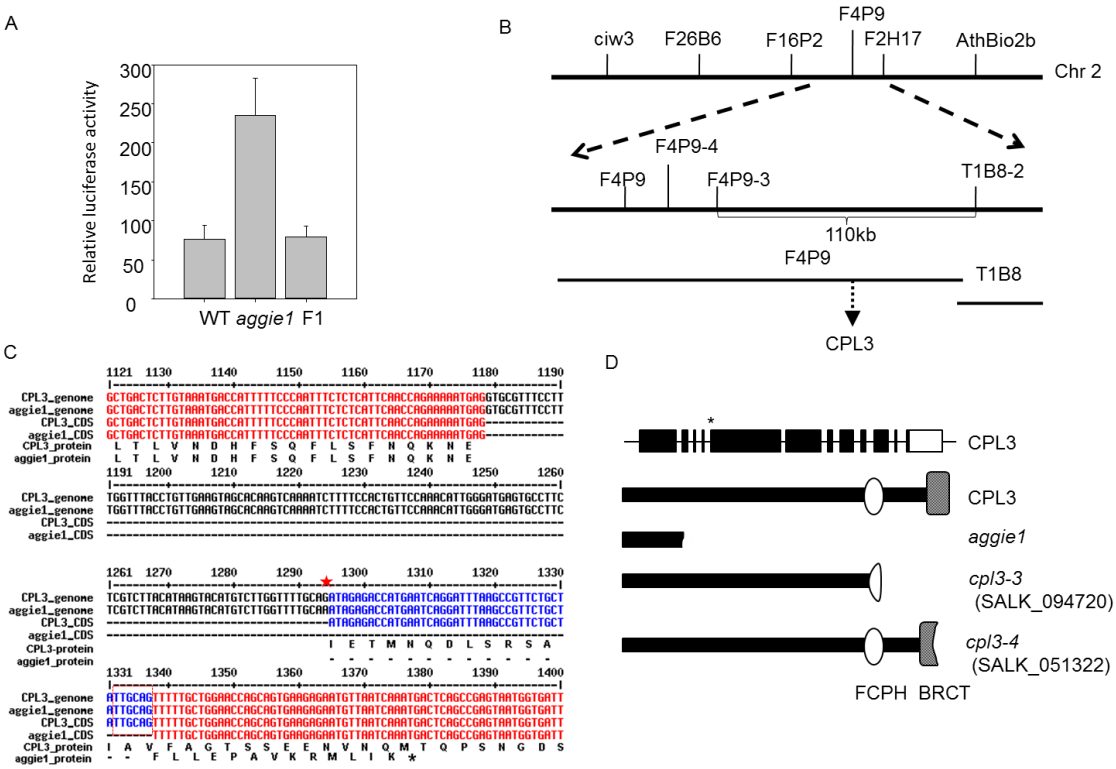

Figure 2.6 *aggie1* was mapped to AT2g33540, a plant CTD phosphatase-like protein. *(A) aggie1* mutant is recessive. The F1 plants crossed from aggie1 and wild type showed similar FRK1::LUC activity under 100nM flg22 treatment (B) Mapping of *aggie1* on chromosome 2 AT2g33540 by using indel markers between marker F4P9-3 and T1B8-2, a 110kb region. (C)Nucleotide acid and amino acid sequence alignment of wild type CPL3 and *aggie1*. Star indicates location of the point mutation. (D) Structure of Aggie1 protein and two other SALK T-DNA insertion alleles *cpl3-3* and *cpl3-4* truncated at FCPH and BRCT domain, respectively.

Aggie1 encodes a plant CTD phosphatase–like protein

Genetic analysis indicated that *aggie1* is a recessive mutant (Figure 2.6A). We crossed the *aggie1* mutants with the polymorphic *Landsberg erecta* and mapped *aggie1* on Chromosome 2 between marker F4P9-3 and T1B8-2 that are 110 kb apart with 310 individual F2 plants displaying *aggie1* phenotypes (Figure 2.6B). We sequenced the

individual genes within this region and identified a G to A mutation in *At2g33540*. The mutation occurs in the 3' splice site of the 4th intron, resulting in a potential alternative 3' acceptor site at 43bp downstream of the original one (Figure 2.6C). *At2g33540* encodes CPL3 with an N-terminal domain, FCPH and BRCT domains. The mutation in *aggie1* results in a truncated protein lacking FCPH and BRCT domains (Figure 2.6D).

To confirm whether the *aggie1* mutants were caused by the mutation in *CPL3* gene, we transformed *CPL3* gene under the control of its native promoter into *aggie1* and tested the *FRK1* promoter activity upon flg22 treatment.*CPL3* gene complemented the *aggie1* mutants and restored the *FRK1* promoter activity to the WT level in the transgenic plants (Figure 2.7A). We also isolated two SALK T-DNA insertion lines *cpl3-3* and *cpl3-4*. Quantitative RT-PCR (qRT-PCR) analysis indicated that endogenous *FRK1* expression was elevated in the *cpl3-4* mutant, consistent with *pFRK1::LUC* activity in *aggie1* mutant (Figure 2.7B). Pathogen growth assays also suggest that *cpl3-3* and *cpl3-4* mutants were more resistant to virulent *P. syringae maculicola* ES4326 (*Psm*) infection than WT plants (Figure 2.7C). Notably, the *cpl2-2* mutant did not alter plant resistance to *Psm* infection, suggesting the differential function of CPL family members in plant immunity (Figure 2.7B)

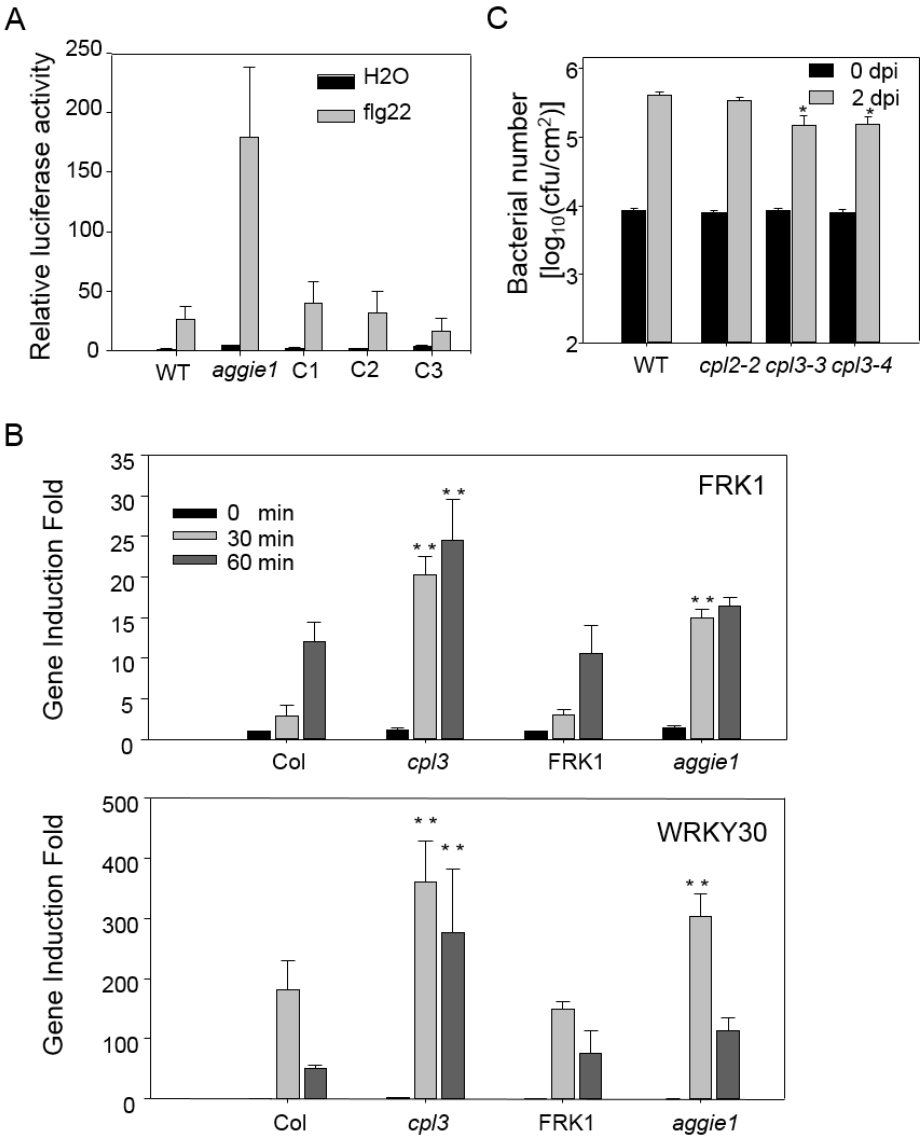

Figure 2.7 AtCPL3 functionally complements *aggie1*. (A) Relative luciferase activity of complementation lines of *aggie1* by transforming with native CPL3 promoter with genomic CPL3 gene. C1, 2, 3 are corresponding complementation line 1, 2, 3. (B) Endogenous FRK1 and WRKY30 expression in *cpl3-4* and Col-0 wild type, *aggie1* and FRK1::LUC transgenic line at 0.5 hour after 100nM flg22 treatment. The data are shown as means ± SEs from three replicates. (C) Bacterial growth assay of *Psm*. Four-week-old *Arabidopsis* plants were inoculated with bacteria at a concentration of 5×10^5 colony-forming units/ml.

CTD phosphorylation dynamics in plant innate immunity

CPLs regulate nuclear gene transcription via modulating the phosphorylation status of the RNAPII CTD. To reveal the potential involvement of CTD phosphorylation in plant innate immunity, we cloned the CTD of *Arabidopsis* RNAPII in a plant expression vector and transfected it into *Arabidopsis* protoplasts. Significantly, flg22 treatment induced a rapid mobility shift of CTD as early as 2 min (Figure 2.8A), and could be removed by calf alkaline intestinal phosphatase (CIP) treatment (Figure 2.8B), suggesting the involvement of phosphorylation in MAMP-induced CTD modification. The phosphorylation pattern of Ser2, Ser5 and Ser7 in CTD heptapeptide conveys a set of informational cues to orchestrate nuclear gene transcription. We examined flg22-induced CTD phosphorylation by using specific antibodies recognizing pSer2, pSer5 or pSer7). To further examine the endogenous CTD phosphorylation dynamics upon flg22 perception, *Arabidopsis* seedlings were treated with flg22 for different time points, and the CTD phosphorylation was detected with α-pSer2, pSer5 or pSer7 antibodies. Flg22 treatment induced Ser2, Ser5 and Ser7 phosphorylation of endogenous CTD of RNAPII (Figure 2.8C). The maximal phosphorylation was observed around 10 to 30 min after treatment and the phosphorylation started to decline 60 min after treatment. The phosphorylation modification was confirmed as the treatment of CIP diminished the signal detected with α-pSer2 antibody (Figure 2.8D). The rapid and transient phosphorylation of CTD by flg22 suggests that phosphorylation dynamics of CTD constitutes an essential step in plant immune signaling.

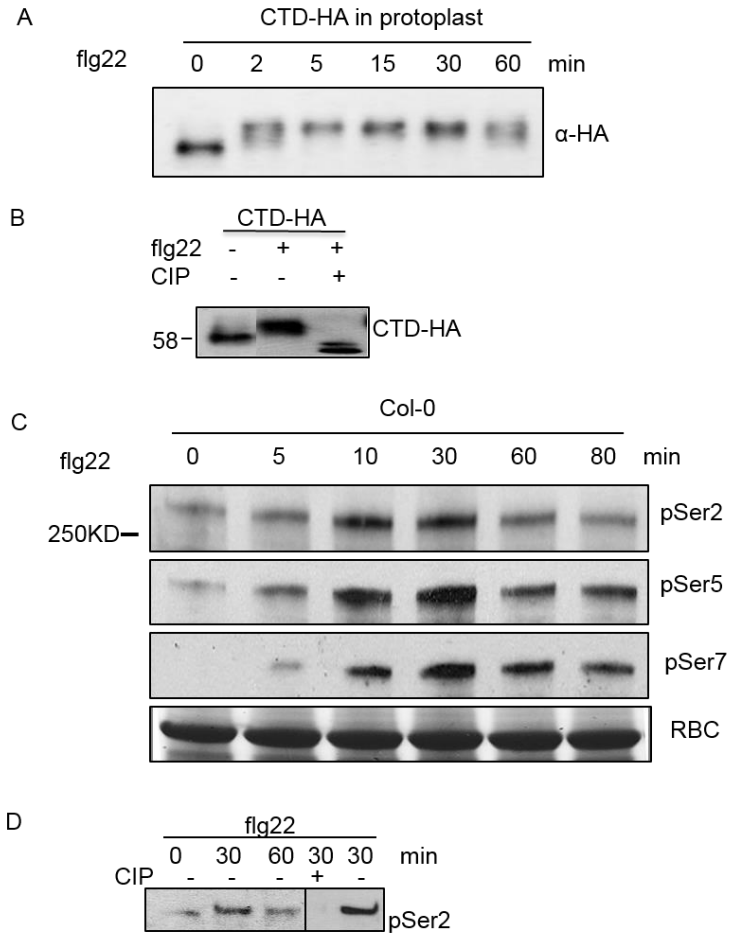

Figure 2.8 Flg22 induced phosphorylation of RNAPII CTD. (A) Mobility shift of RNAPII CTD under flg22 treatment in *Arabidopsis* protoplast. HA tagged CTD domain construct was transfected into Arabidopsis protoplast for overnight, and then treated with 100nM flg22 for indicating time points. Western was performed with HA antibody. (B) The Mobility shift of RNAPII CTD could be removed by CIP. (C) 10-day old seedlings were transferred from 1/2 MS medium into water for overnight, and then treatment with 100nM flg22 for indicating time points. Total proteins were extracted and western blot was performed as described in Material and methods. (D) Phosphorylation of endogenous RNAPII could be removed by CIP.

CPL3 localizes to the nucleus

In order to function directly on RNAPII, CPL3 should localize in nucleus. Based on bioinformatic (NLS mapper) prediction, there is a nuclear localization signal in the middle of CPL3, close to N-terminal region (Figure 2.9A). CPL4, the closest homolog of CPL3 in Arabidopsis, have the conserved NLS signal with CPL3. Thus we fused CPL3, CPL3N-terminus (CPL3N), and CPL3C-terminus (CPL3C) (Figure 2.9A) with a GFP tag on their C terminus, and transfected into *Arabidopsis* protoplasts. From microsopic image, we can clearly see the CPL3N, and CPL3 full-length protein localized in nucleus, overlapping with the nucleus localization signal (NLS)-RFP control; whereas CPL3C spreaded in the cytosol. (Figure 2.9B). The GFP signal of CPL3 and CPL3N was observed during 0.5 to 2 hours with and without flg22 treatment, and the nuclear localization did not change throughout the duration of the experiment. This result provided the evidence that CPL3 localizes in nucleus, and could potentially function as a RNA PolII regulator.

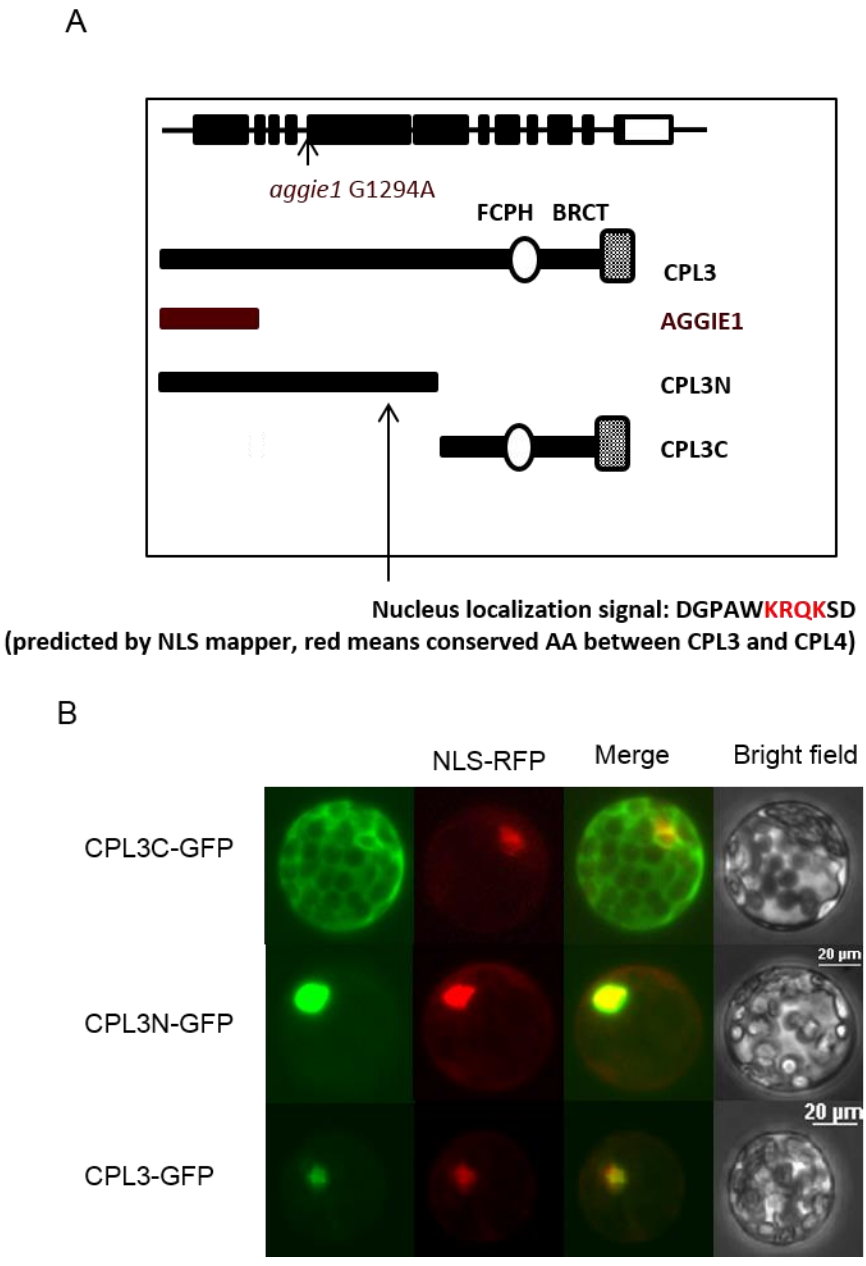

Figure 2.9 CPL3 locates to the nucleus. (A) Structure of CPL3, and AGGIE1 gene. (B) C-terminal, N-terminal and full length CPL3 GFP fusion were transfected into *Arabidopsis* protoplast cells. Protoplasts were observed 12 *hpt* with a confocal microscopy. Nuclear-localized RFP was co-transfected as nucleus-location control.

Aggie1 specifically dephosphorylates the RNAPII CTD Ser2 in vitro and in vivo

Our data reveal an interesting CTD phosphorylation dynamic upon PAMP signal perception. We further tested whether CPL3 (the causal mutation of *aggie1*) could directly modulate CTD phosphorylation status to regulate immune gene expression. We purified maltose-binding protein (MBP) fusion proteins of full-length CPL3, CPL3N and CPL3C and performed *in vitro* phosphatase assays. The glutathione-S-transferase (GST) fusion proteins of CTD were phosphorylated by active *Arabidopsis* MPK3, and the phosphorylation status of CTD was detected by specific α-pSer2, pSer5 or pSer7 antibodies. Significantly, CPL3 could specifically dephosphorylated pSer2, not pSer5 or pSer7 *in vitro* (Figure 2.10A). As expected, CPL3C which contains FCPH and BRCT domains, not CPL3N which lacks these domains, carries the specific phosphatase activity of dephosphorylating pSer2 (Figure 2.10A). We also compared Ser2 and Ser5 phosphorylation level of endogenous CTD in WT and *aggie1* seedlings treated with flg22. Consistent with the *in vitro* assay, the overall Ser2 phosphorylation level was enhanced in the *aggie1* mutants compared to WT plants with and without flg22 treatment (Figure 2.10B). In contrast, the level of Ser5 phosphorylation is similar in WT and *aggie1* seedlings (Figure 2.10B). The data provide genetic and biochemical evidence that CPL3 is a specific CTD Ser2 phosphatase. Apparently, CPL3 preferentially counteracts MAMP-triggered phosphorylation of CTD Ser2 to negatively regulate immune gene activation and disease resistance.

Both FCPH and BRCT domains are required for yeast FCP1 catalytic activity. Among 20 *Arabidopsis* CPL genes, only CPL3 and CPL4 contain both FCPH and BRCT domains. We tested whether BRCT domain is required for CPL3 phosphatase activity. The CPL3 FCPH domain lacking BRCT domain was unable to dephosphorylate pSer2 of CTD in an *in vitro* phosphatase assay (Figure 2.10A). The data suggest that the BRCT domain is required for CPL3 phosphatase activity, consistent with yeast FCP1 function.

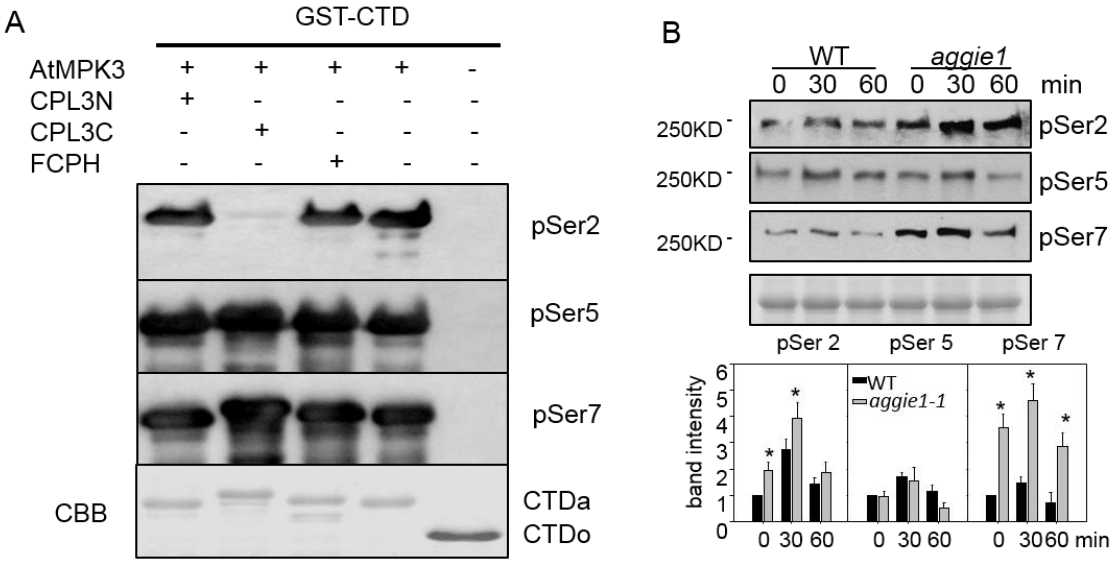

Figure 2.10 CPL3 dephosphorylates RNAPII CTD *in vitro* and *in vivo.* (A) Phosphorylation and dephosphorylation of RNAPII CTD *in vitro.* Purified active MAPK3 were used to phosphorylate CTD-GST, and after replacing kinase buffer to phosphatase buffer, C terminus, N terminus, or FCP domain of CPL3 were added and incubated. Western blot was performed with specific pSerine antibody for RNAPII. (B) Phosphorylation of RNAPII CTD *in vivo* was analyzed by using wild type and *aggie1* mutants. Wild type plant seedlings and the *aggie1* mutant seedlings were with 100nM flg22 for indicating time points, and western blot with specific phospho-Ser antibodies were performed to detect phosphorylation status of endogenous RNA Polymerase II.

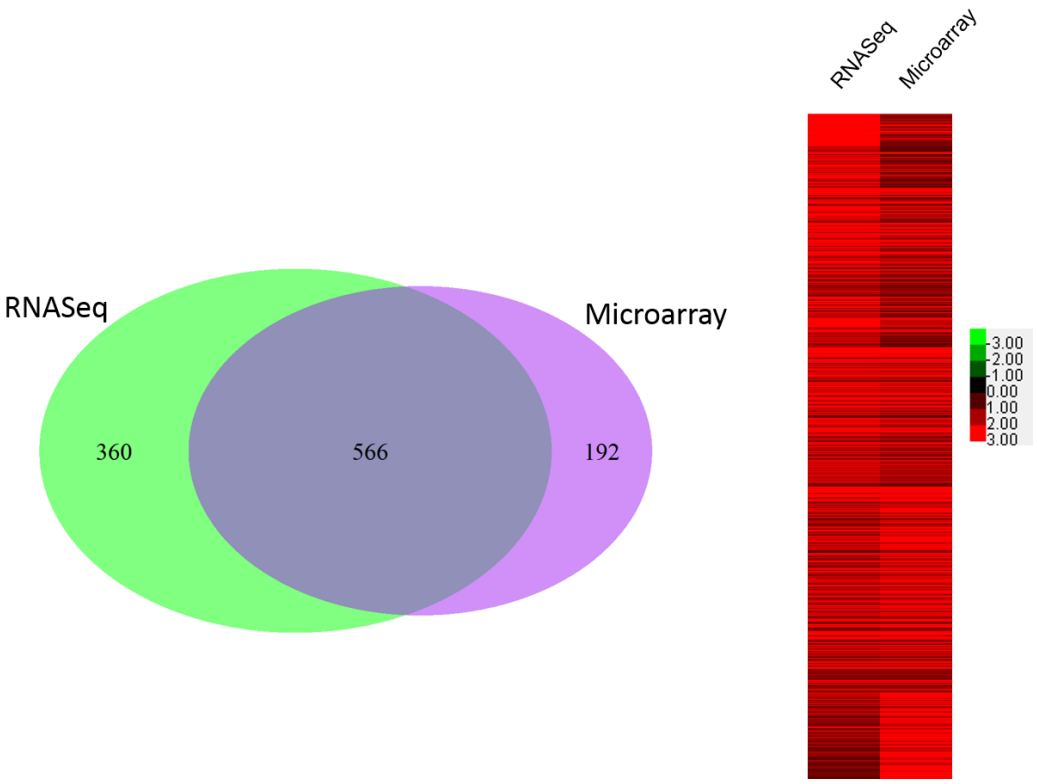

Figure 2.11. Comparison of RNA-seq and Microarray data for flg22-induced transcriptome. (A) Van diagram of flg22-induced genes (2 fold changes) between published microarray and RNA-seq results (RPKM>1). Graph was generated with R software (B) Heat map of flg22-induced genes (2 fold changes) between published microarray and RNA-seq results (RPKM>1). Graph was generated with Cluster 3.0 and Treeview software.

cpl3 has enhanced flg22-induced transcriptome

RNA polymerase II directly controls transcription of DNA to synthesize precursors of mRNA. Since CPL3 modifies the phosphorylation status of the RNAPII CTD, which directly affects RNAPII transcription capacity, we applied RNA sequencing analysis to determine the influence of CPL3 on the global transcriptome between WT and

the *cpl3* mutant. We first compared the RNA sequencing (RNA-seq) data with two published microarrays with similar experimental conditions (Marie Boudsocq et al., 2010; Cyril Zipfel et al., 2004). RNA-seq data provides a similar list of induced genes compared with the two published microarray data sets when we used strict filter standard (RPKM>1, stands for total reads >100) (Figure 2.11A, B). By comparing the transcription expression ratio between WT and *cpl3* seedlings without any treatment, no dramatic changes were observed on detected transcripts (Figure 2.12A). This suggests that CPL3 did not affect general transcription capacity of RNAPII. We then compared the flg22-mediated transcriptome in *cpl3* with wild type. There are 1002 genes that were induced more than two fold for wild type under flg22 treatment (RPKM>1, stands for total reads number >100) whereas there were 1788 genes in *cpl3*. Among these induced genes, 877 genes (88%) overlap between wild type and the *cpl3* mutant. Significantly, the induction intensity appears to be exacerbated in cpl3-3 mutant than that in Col-0 with 543 of 877 (62%) overlapping genes induced more than 1.5 fold in cpl3-3 mutant (Figure 2.12B). This indicates that CPL3 negatively regulated flg22-mediated PTI transcriptional changes. We applied quantitative real time PCR to validate part of RNA-seq data, and here we show that AT1g07160, AT2G17740, AT1G51920, AT1G59865, AT1G59860 have the enhanced expression in both aggie1 and cpl3 mutants under flg22 treatment, consistent with the RNA-seq data (Figure 2.12C). This result is consistent with previous data, and validates that CPL3 is indeed a negative regulator in PTI pathway.

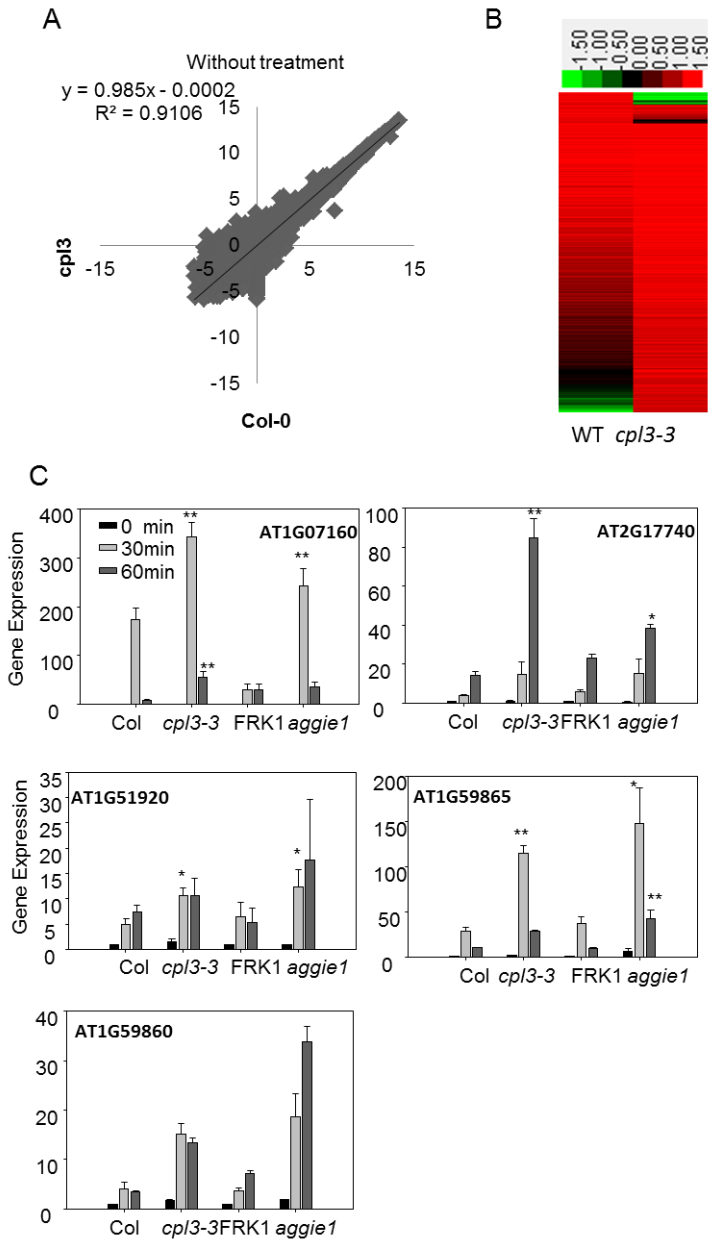

Figure 2.12 RNA-seq analysis of *cpl3* under flg22 treatment. (A) Scatter plot with global transcripts expression between wild type and cpl3 mutants without treatment. Graph was generated with Excel 2010 (Microsoft). (B) Heatmap for flg22-induced genes with 2 fold induction in either WT or cpl3 mutants at 30mins after treatment. Graph was generated with Cluster 3.0 and Treeview software. (C) RT-PCR validation of RNA seq results for representative genes. The data are shown as means ± SEs from three biological replicates with Student's T-test. (* indicates $p<0.05$, ** indicates $p<0.01$).

CDKC gene family

Since RNA Polymerase II could be phosphorylated under flg22 treatment, and CPL3 is an RNAPII CTD serine 2 phosphatase, playing a negative role on PTI signaling, it is reasonable to test the function of Ser 2 CTD kinases (CDKs) on PTI pathway. CTD kinases such as P-TELF-b (positive elongation factor b) could phosphorylate Ser 2 residue of RNAPII and release the pausing of the RNAPII into elongation steps. The P-TELF-b has two subunits: CDK9 and cyclin T. In Arabidopsis, CDK9 has two homologs: AtCDKC1 and AtCDKC2 (Guo & Stiller, 2004; Sim, Belotserkovskaya, & Reinberg, 2004). CDKC1 and CDKC2 and their interacting partners were reported to play important roles in infection with Cauliflower mosaic virus (CaMV). The *cdkc2* and *cyc.;1-5* double KO plants were extremely resistant to CaMV (Cui, Fan, Scholz, & Chen, 2007).

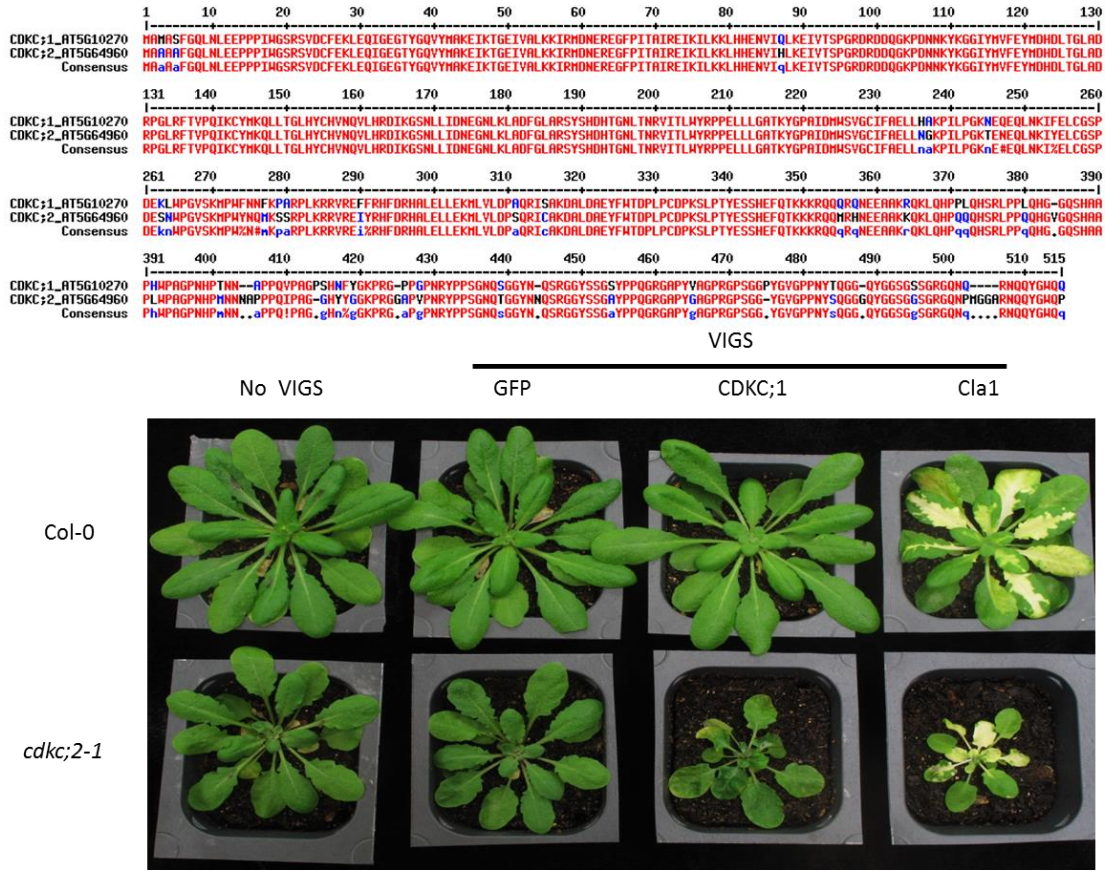

Figure 2.13 Sequence alignment of CDKC1 and CDKC2 and phenotype of VIGS Cdkc1 on wild type and *cdkc;2* mutants. (A) Amino acid alignment between AtCDKC1 and AtCDKC2. (B) Phenotype of VIGS Cdkc1 on wild type (Col-0) and *cdkc2-1* mutants. 2 weeks old plants were inoculated with Agrobacteria containing VIGS vector (as described in Material and Methods). The picture was taken 3 weeks after inoculation.

The CDKC1 and CDKC2 have high sequence similarity (Figure 2.13A). The T-DNA insertion lines of *cdkc*1 still have CDKC1 transcripts tested by RT-PCR, indicating they are not complete knock out mutants. Alternatively, we applied virus-induced gene silencing technology to silence CDKC1 in both Col-0 and *cdkc2-1* background. After

silencing CDKC1 in *cdkc2-1*, the plants grow dramatically slow and leaves showed severe curved phenotype (Figure 2.13B). Firstly we checked the RNA polymerase II phosphorylation status in the VIGS *cdkc1* silencing plants compared with the control (Figure 2.14), and the phosphorylation status of RNA PolII was significantly decreased in *cdkc1* and *cdkc2* double mutants, and was slightly decreased in *cdkc1* or *cdkc2* single mutants.

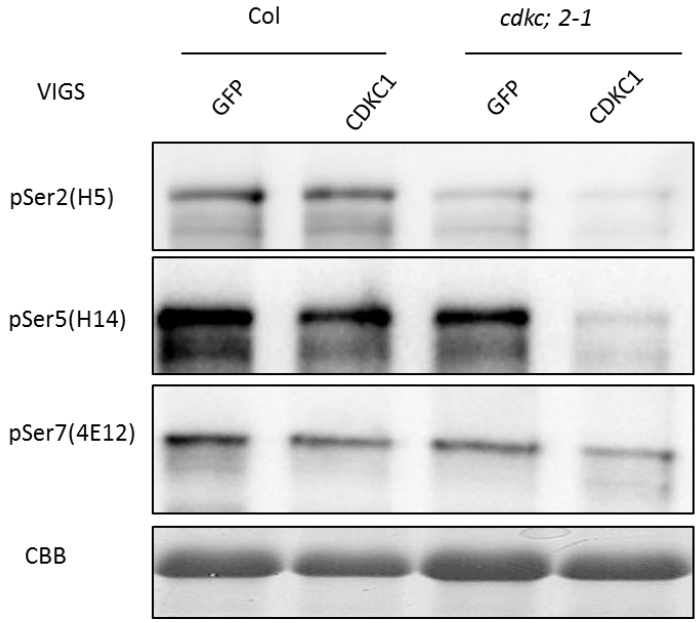

Figure 2.14 Phosphorylation of RNA Pol II was attenuated in *cdkc1, cdkc2* mutants. Total proteins were extracted from plants with VIGS of Cdkc1 on Col and *cdkc2-1*. Western blot was performed with specific pSerine antibody.

We then tested the flg22 induced transcription expression in *cdkc1*, *cdkc2* single mutants and double mutants (Figure 2.15A). The FRK1 induction was dramatically

reduced in *cdkc1*, *cdkc2* single mutants, and even more severe in double mutants. A similar trend was observed for another marker gene WRKY30. Significantly, from the bacterial growth assay *in planta* by using virulent strain *Pst* DC3000, the bacteria grew 10 times more in double mutants and grew about 5 times more in the single mutants (Figure 2.15B). All the data above suggests that CDKC1 and CDKC2 play a positive role in PTI signaling.

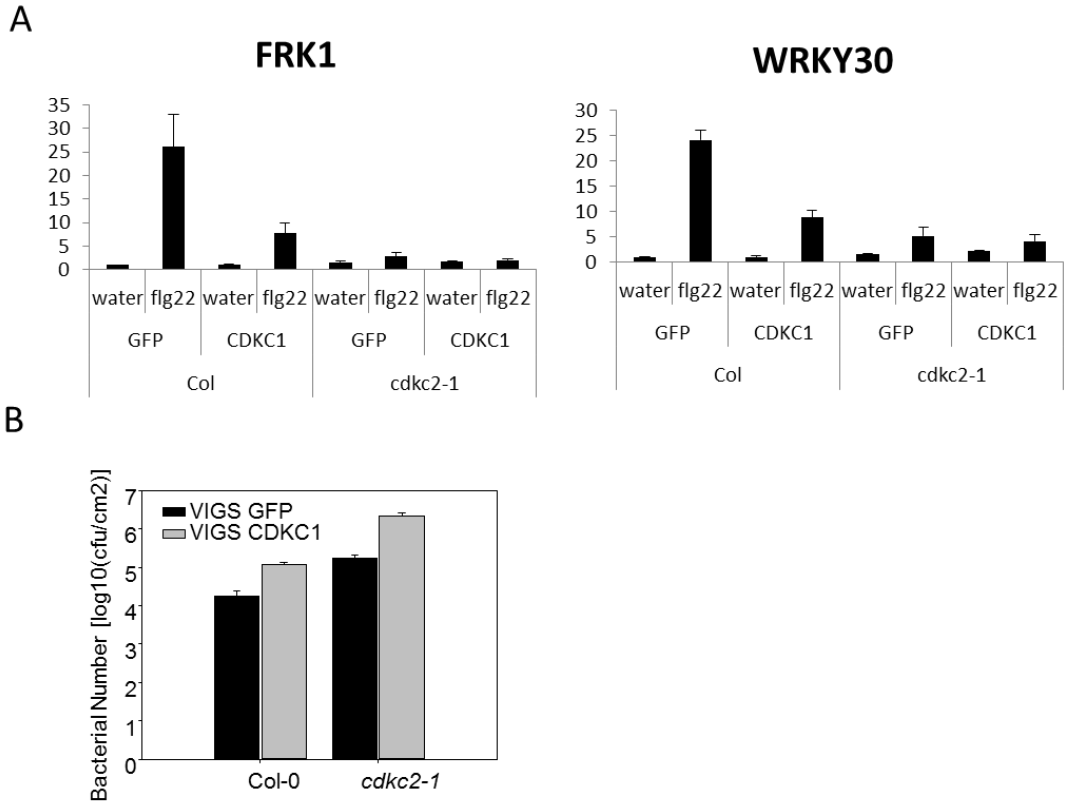

Figure 2.15 Defense responses were attenuated in *cdkc1* and *cdkc2* mutants. (A) FRK1 and WRKY30 transcription expression in VIGS of Cdkc1 on Col-0 and *cdkc2-1* plants under flg22 treatment. 100nM flg22 was hand inoculated into plants' leaves and harvested 3 hours after inoculation. Data was shown as three biological repeats. The error bar standands for standard error between three repeats. (B) Bacterial growth assay for VIGS of Cdkc1 on Col-0 and *cdkc2-1* plants. The plants were hand-inoculated with *Pst* DC3000 at 2 x 10^8 cfu/ml and bacterial growth assay were performed 4th day after inoculation.

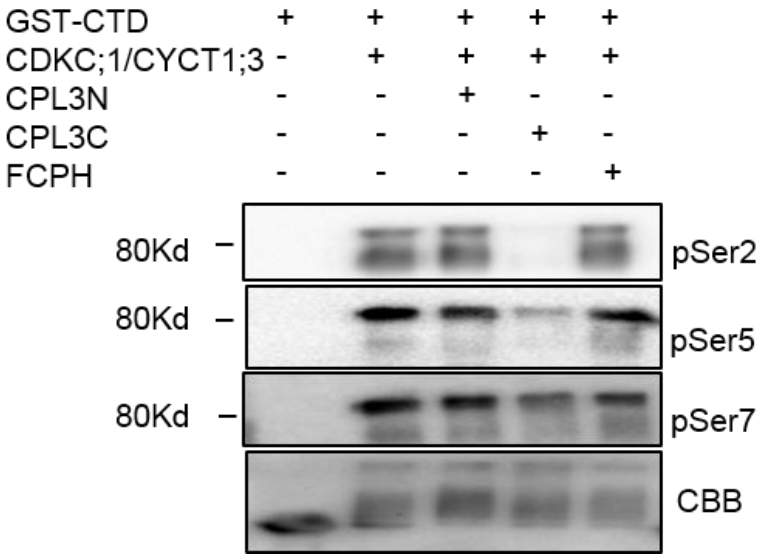

Figure 2. 16 CPL3 dephosphorylates CDKC1/2 phosphorylated RNA polymerase II CTD *in vitro.* Purified CDKC1 or CDKC2 and CYCT1;3 were used to phosphorylate CTD-GST, and after replacing kinase buffer to phosphatase buffer, C terminus, N terminus, or FCP domain of CPL3 were added and incubated. Western blot was performed with specific phosphorylated serine antibody for RNA PII.

CDKC1/2 phosphorylate RNA polymerase II CTD

Our data reveal an interesting CTD phosphorylation dynamic upon MAMP signal perception. We further tested whether CPL3 (the causal mutation of *aggie1*) could directly modulate CTD phosphorylation status to regulate immune gene expression. We purified MBP fusion proteins of full-length CPL3, N-terminal CPL3 (CPL3N) and C-terminal CPL3 (CPL3C) and performed *in vitro* phosphatase assays. We purified MBP fusion proteins of full-length CDKC1 CDKC2 and performed *in vitro* phosphorylation assays. To our expectation, the GST fusion proteins of CTD were phosphorylated by active CDKC1 and CDKC2, and the phosphorylation status of CTD was detected by specific α-

pSer2, pSer5 or pSer7 antibody. Significantly, CPL3 could specifically dephosphorylated pSer2, and slightly on pSer5, pSer7 *in vitro* (Figure 2.16). As expected, CPL3C which contains FCPH and BRCT domains, not CPL3N with unknown function, carries the specific phosphatase activity of dephosphorylating pSer2 (Figure 2.16).

Discussion

During millions of years, bacterial pathogens and plant hosts have evolved invasion and defense systems to counteract with each other. During this arms race evolutionary interaction between pathogens and plant hosts, the latter obtained the membrane receptors to recognize essential components from pathogens as an alarm signal, such as, lipopolysaccharide (LPS) from Gram-negative bacterial, flagella, and elongation factor Tu. Although much research has been done in this field, large amounts of components and the genetic networks are still incomplete. Here, we took advantages of promoter-luciferase system and applied forward-genetic strategy to identify the unknown components in this signaling pathway. The first component we identified is CPL3, encodes a RNA polymerase II CTD phosphatase. We showed here that CPL3 dephosphorylates RNA polymerase II CTD, which affects RNA polymerase II transcription capacity in flg22-mediated signaling pathway (Figure 2.17).

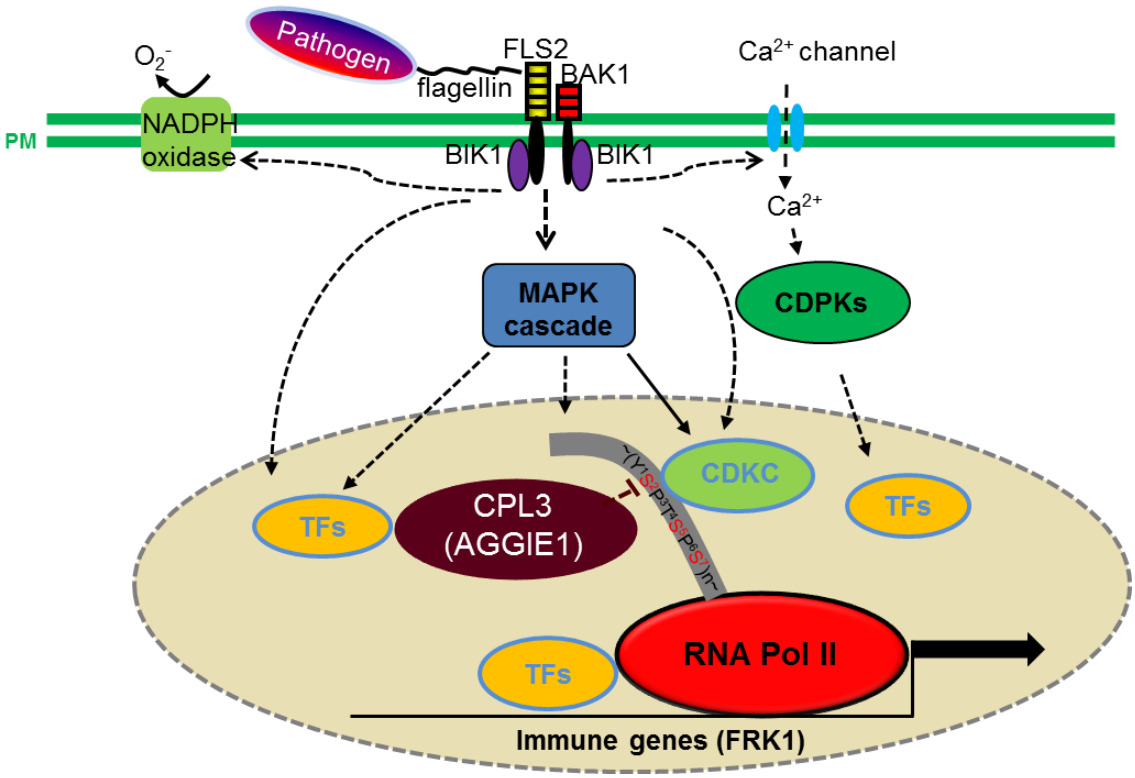

Figure 2.17 Proposed model of the role of AGGIE1 in plant immunity. When the bacterial pathogen infects the plant host, the flagella could be perceived by cell membrane receptor FLS2, and co-receptor BAK1, and activate the downstream MAPK cascades and CDPKs. RNA polymerase II CTD could be further phosphorylated under flg22 treatment. CDKC kinases and CPL3 (AGGIE1) function as CTD kinases and phosphatases separately, playing orchestrated roles to regulate flg22-mediated transcriptional changes.

The synthesis of mRNAs in eukaryotes is accomplished by RNA polymerase II (RNAPII). The largest subunit of RNA polymerase II, Rpb1, has a flexible C terminal domain (CTD) consisting of tandemly repeated heptapeptide: $Y^1S^2P^3T^4S^5P^6S^7$. The number of repeats is variable from 34 in yeast to 52 in mammals. In *Arabidopsis*, there are 42 repeats. 5 residues out of heptapeptides could be post-translational modified:

tyrosine, serine and threonine could be phosphorylated. Proline could have cis and trans isoforms, which might play important roles in the structure and function of CTD. The modification of these residues in each repeat is essential but complicated, making CTD an important regulator for transcription cycle. CTD is dispensable for RNA polymerase enzyme activity *in vitro*, but deletion of entire CTD is lethal in yeast, mice or drosophila, suggesting the important function of CTD.

Serine 2 and 5 are two residues studied extensively in the last decade. Phosphorylation of Ser5 is crucial for release of RNA polymerase pausing at the 5' of a coding gene, and mutation of ser5 to glutamic acid at proximal residue makes yeast lethal, indicating an essential role for phosphorylation of Ser5. Phosphorylation of Ser 2 is considered as a mark for transcription elongation; however, mutation of all the Ser 2 to alanine was tolerated, but delay in colony formation in yeast, indicating phosphorylation of serine 2 is not essential for vegetative growth (Coudreuse, et al., 2010). *In vivo*, Ser5 kinase is principally TFIIH (Kin28 in yeast, and CDK7 metazoans), and interestingly, Ser5 could be phosphorylated by signal-related kinase Erk1/2, by which RNAPII CTD could be turned into a hyperphosphorylated form, suggesting this event might be signal dependent (Bonnet, et al., 1999). Serine 2 residue is mainly phosphorylated by CTDK-I (CDK9 in metazoans). Importantly, the dynamics of dephosphorylation of Ser2 and Ser5 are considered as an important regulator of transcription cycle and RNAPII recycling. FCP1, an evolutionarily conserved protein, could preferentially dephosphorylate pSer2 and Ssu72 in yeast and SCP1 in mammals could preferentially dephosphorylate pSer5.

FCP1 is essential for yeast viability, and abrogation of Ssu72 makes transcription defect and increase of phosphorylated Ser5.

We showed here that CPL3 preferentially dephosphorylates Ser2 residue *in vivo* and *in vitro*. The *cpl3* mutants showed enhanced flg22 mediated transcriptome changes by using whole transcriptome analysis, but not general transcriptional changes. The homolog of CPL3 in *Arabidopsis*, CPL4, plays important role in general transcriptional regulation. CPL4, lacking, the long N terminal domain of CPL3, only contains the two functional domains FCPH and BRCT. CPL4 RNAi lines are extremely dwarfed, and T-DNA insertion lines are not available, indicating that CPL4 might be essential for plant growth. The long N terminal domain of CPL3 might play essential role for CPL3's function.

We also found that CDKC1 and CDKC2, the kinases for RNA polymerase II, could phosphorylate RNA polymerase II on 3 serine residues *in vivo* and *in vitro*. The *cdkc1 cdkc2* mutants had attenuated immune signaling and compromised to bacterial pathogen, indicating their positive role in PAMP-triggered immune signaling pathway. It would be worthwhile to identify the upstream signaling above CDKC1/2. It might be MAPK kinases or CDPKs that potentially enhance the phosphorylation of RNA polymerase II CTD.

CHAPTER III

PLANT IMMUNE RESPONSE TO PATHOGENS DIFFERS WITH CHANGING TEMPERATURES*

Summary

Temperature fluctuation is a key determinant for microbial invasion and host evasion. In contrast to mammalians that maintain constant body temperature, plant temperature oscillates on a daily basis. It remains elusive how plants operate inducible defenses in response to temperature fluctuation. We report that ambient temperature changes lead to pronounced shifts of two distinct plant immune responses: pathogen-associated molecular pattern (PAMP)-triggered immunity (PTI) and effector-triggered immunity (ETI). Plants preferentially activate ETI signaling at relatively lower temperatures [1] (10~23°C), whereas switch to PTI signaling at moderately elevated temperatures (23~32°C). The *Arabidopsis arp6* and *hta9hta11* mutants, phenocopying plants grown at the elevated temperatures, exhibit enhanced PTI and yet reduced ETI responses. As the secretion of bacterial effectors favors low temperatures whereas bacteria multiply vigorously at elevated temperatures accompanied with increased MAMP production, our findings suggest that temperature oscillation might have driven dynamic

---

*Reprinted with permission from "Plant immune response to pathogens differs with changing temperatures" by C. Cheng, X. Gao, B. Feng, J. Sheen, L. Shan & P. He *Nature Communications*, 2013 Sep 26;4:2530.

co-evolution of distinct plant immune signaling responding to pathogen physiological changes.

Introduction

Innate immunity is triggered by the activation of immune receptors through detection of non-self components. The first line of innate immunity is initiated by the detection of pathogen or microbe-associated molecular patterns (PAMPs or MAMPs) through pattern recognition receptors (PRRs). In plants, MAMPs are perceived by cell-surface receptor-like kinases (RLKs) to mount pattern-triggered immunity (PTI) (Boller & Felix, 2009; Monaghan & Zipfel, 2012). Bacterial flagellin and elongation factor Tu (EF-Tu) are perceived by leucine-rich repeat RLK (LRR-RLK), FLS2 and EFR respectively (Gomez-Gomez & Boller, 2000; Zipfel et al., 2006). Upon ligand perception, FLS2 and EFR rapidly associate with another LRR-RLK BAK1, thereby initiating downstream signaling (Chinchilla et al., 2007; Heese et al., 2007). A receptor-like cytoplasmic kinase BIK1 is quickly phosphorylated upon flagellin or EF-Tu perception. BIK1 is associated with FLS2/BAK1 and EFR/BAK1 receptor complexes and is directly phosphorylated by BAK1 (Lu et al., 2010; Zhang et al., 2010). MAPK (mitogen-activated protein kinase) cascades and CDPKs (calcium-dependent protein kinases) act downstream of LRR-RLK receptor complexes in transducing intracellular signaling events, which ultimately lead to transcriptional reprogramming (Asai et al., 2002; Boudsocq et al., 2010). PTI signaling could be down-regulated by turnover of PAMP receptors. Two E3 ubiquitin

ligases PUB12 and PUB13 interact with and ubiquitinate FLS2 receptor for proteosome-mediated degradation upon flagellin perception (Lu et al., 2011).

Successful pathogens are able to suppress PTI by producing virulence effectors. In particular, many pathogenic bacteria deliver a plethora of effector proteins into host cells through type III secretion system (T3SS) to favor pathogen survival and multiplication. Many of these effectors target important host components to sabotage host immune responses and physiology (Block & Alfano, 2011; Feng et al., 2012). To confine or eliminate pathogens, plants further evolved intracellular nucleotide-binding domain leucine-rich repeat (NLR) proteins to directly or indirectly recognize effectors and initiate effector-trigger immunity (ETI) (Dodds & Rathjen, 2010; Spoel & Dong, 2012). Plant NLR proteins share structural similarity with mammalian NOD-like receptors that perceive intracellular PAMPs and danger signals to initiate inflammation and immunity (Maekawa, Kufer, & Schulze-Lefert, 2011). The *Pseudomonas syringae* effector AvrRpt2 is recognized by the *Arabidopsis* NLR protein RPS2 whereas two sequence-unrelated effectors, AvrRpm1 and AvrB are recognized by RPM1 to initiate ETI responses including transcriptional reprogramming, hypersensitive response (HR) such as reactive oxygen species (ROS) production. Instead of direct NLR-effector interaction, RPS2 and RPM1 monitor the perturbation of the host protein RIN4 targeted by pathogen effectors to mount defense responses (Axtell & Staskawicz, 2003; Mackey et al., 2003). Specific CDPKs downstream of NLR proteins sense sustained increase of cytosolic Ca^{2+} concentration and regulate the PTI or ETI defense responses via phosphorylation of different substrates and subcellular dynamics (Gao et al., 2013).

Environmental factors often have profound impacts on microbial invasion and host evasion (Wang et al., 2011). Temperature fluctuates both daily and seasonally has long been considered as one of key determinants for disease epidemics (Alcazar & Parker, 2011; Murdock, Paaijmans, Cox-Foster, Read, & Thomas, 2012). In many cases, virulence genes of mammalian pathogens are induced at 37°C, which is a typical body temperature of mammalians, but are repressed below 30°C (Konkel & Tilly, 2000). Accordingly, elevating mammalian body temperature to fever range results in an increase of MAMP-induced downstream signaling (Lee, Zhong, Mace, & Repasky, 2012). In contrast, many virulence effector proteins in plant pathogenic bacteria are induced at 16-24°C and repressed above 28°C (Smirnova et al., 2001; van Dijk et al., 1999; Wei, Sneath, & Beer, 1992). For instance, *P. syringae* effectors HrmA and AvrPto were secreted at their highest amounts when the temperature was between 18°C and 22°C (van Dijk et al., 1999). The production of *P. syringae* phytotoxin coronatine is also temperature sensitive: induced at 18°C and repressed at 28°C (Ullrich, Penaloza-Vazquez, Bailey, & Bender, 1995). Plant body temperature fluctuates with their living environment on a daily basis. It remains unknown whether and how plants integrate ambient temperature oscillations with regulation of inducible defense programs triggered by distinct pathogen components.

Material and methods

Plant growth conditions, chemical treatments and bacterial inoculation

Arabidopsis wild-type (Col-0), *arp6-10* and *hta9 hta11* mutant plants were grown in pots containing soil (Metro Mix 360) in a growth room at 23°C, 60% relative humidity

and 75 μE m^{-2} s^{-1} light with a 12 hr photoperiod for approximate 4 weeks before protoplast isolation, bacterial inoculation or different temperature treatments. The *arp6-10* and *hta9 hta11* mutant seeds were obtained from Dr. P. Wigge in John Innes Centre. The temperature treatments were performed in different growth chambers set at the indicated temperature for certain time.

Pst, *Pst avrRpm1* or *avrRpt2* strains were grown overnight at 28°C in the KB medium containing rifamycin (50 μg ml^{-1}) or in combination with kanamycin (50 μg ml^{-1}). Bacteria were pelleted by centrifugation, washed, and diluted to the desired density. The leaves were hand-inoculated with bacteria using a needleless syringe, collected at the indicated time for bacterial counting, cell death staining, electrolyte leakage assays or for RNA isolation. To measure bacterial growth, two leaf discs were ground in 100 μl H_2O and serial dilutions were plated on KB medium with appropriate antibiotics. Bacterial colony forming units (cfu) were counted 2 days after incubation at 28°C. Each data point is shown as triplicates.

At least three independent repeats were performed for all experiments. The representative data with similar results were shown. The statistical analysis was performed with SPSS software (SPSS Inc., Chicago).

Protoplast transient assay

Protoplast isolation and transient expression assay were conducted as described (X. Gao et al., 2013; Dongping Lu et al., 2010). In general, 50 μl protoplasts at the density of 2 x 10^5 /ml and 10 μg DNA were used for promoter activity, 100 μl protoplasts and 20 μg

DNA were used for protein expression and 500 µl protoplasts and 100 µg DNA were used for RT-PCR analyses. For reporter assay, *pUBQ10::GUS* was co-transfected as an internal transfection control, and the promoter activity was presented as LUC/GUS ratio. Protoplasts transfected with empty vector were used as a control.

MAPK activity and BIK1 phosphorylation assays

To detect MAPK activity, 10-day-old WT, *hta9/hta11* and *arp6-10* seedlings grown on 1/2MS medium were transferred to water for overnight and then treated with 100 nM flg22 or H_2O for indicated time points and frozen in liquid nitrogen. The seedlings were homogenized in an extraction buffer containing 50 mM Tris-HCl, pH7.5, 100 mM NaCl, 15 mM EGTA, 10 mM $MgCl_2$, 1 mM NaF, 0.5 mM $NaVO_3$, 30 mM β-glycerophosphate, 0.1% IGEPAL, 0.5 mM PMSF, 1% protease inhibitor cocktail. Equal amount of total protein was electrophoresed on 10% SDS–PAGE. An α-pERK antibody (Cell Signaling) was used to detect phosphorylation status of MPK3 and MPK6 with an immunoblot. For different temperature treatments, the seedlings were pretreated at different temperatures for 15 min and then treated with 100 nM flg22 or H_2O for 10 min. For BIK1 phosphorylation assay, *Arabidopsis* protoplasts were transfected with HA epitope-tagged BIK1 and incubated at room temperature for overnight, pre-treated at 16, 23, or 28°C for 15 min and then treated with 100 nM flg22 or H_2O for 10 minutes. Total protein was separated by 10% SDS–PAGE gels followed by an α-HA immunoblot.

RIN4 degradation and phosphorylation in planta

Dex-inducible AvrRpt2-HA (in Col background) transgenic plants were obtained from Dr. Fred Ausubel. The 3 week-old transgenic plants were pretreated at 23 or 32C° for 1 hour and then inoculated with 10μM DEX or H_2O for 8 hours and frozen in liquid nitrogen. The samples were homogenized in an extraction buffer containing 50 mM Tris-HCl, pH7.5, 100 mM NaCl, 15 mM EGTA, 10 mM $MgCl_2$, 1 mM NaF, 0.5 mM $NaVO_3$, 30 mM β-glycerophosphate, 0.1% IGEPAL, 0.5 mM PMSF, 1% protease inhibitor cocktail. Equal amount of total protein was electrophoresed on 15% SDS–PAGE. An RIN4 antibody with 1:500 dilution (gift from Dr. Gitta Coaker) was used to detect RIN4 with an immunoblot. HA antibody was used to detect AvrRpt2 and AvrRpm1 with an immunoblot.

Cell death assays

For HR assays, the leaves of 4-week-old plants were hand-inoculated with 10 μM DEX or different bacteria at 1 x 10^8 cfu/ml, and the cell death was calculated as the percentage of wilting leaves to total leaves inoculated.

For trypan blue staining, leaves of *DEX-AvrRpt2* plants were inoculated with H_2O or 10 μM DEX, and collected at 24 *hpi* after treatment. The leaves were stained with trypan blue in lactophenol (Lactic acid: glycerol: liquid phenol:distilled water=1:1:1:1) solution, then destained with 95% ethanol/lactophenol solution, and washed with 50% ethanol. For electrolyte leakage assays, five leaf discs (0.5 cm diameter) were excised from the WT or mutants infiltrated with bacteria and pre-floated in 10 ml of ddH_2O for

10~15 min to eliminate wounding effect. The ddH_2O was then changed and electrolyte leakage was measured using a conductivity meter (VWR; Traceable Conductivity Meter) with three replicates per time point per sample.

RT-PCR and qRT-PCR analysis

Total RNA was isolated from leaves or protoplasts with TRIzol Reagent (Invitrogen). One μg of total RNA was used for complementary DNA (cDNA) synthesis with oligo (dT) primer and reverse transcriptase (New England BioLabs). qRT-PCR analysis was carried out using iTaq SYBR green Supermix (Bio-Rad) supplemented with ROX in an ABI **GeneAmp® PCR System 9700**. The expression of PTI and ETI marker genes was normalized to the expression of *UBQ10*. The regular RT-PCR was performed with 35 cycles. The primer sequences were reported or listed in Table 2.

Table 2. Primers used in temperature project

qRT-PCR primers

Gene	Forward primer	Reverse primer
At2g17740	TGCTCCATCTCTCTTTGTGC	ATGCGTTGCTGAAGAAGAGG
At1g07160	CGTGTTGGGGATTGATTCG	AGAGCTCGGGCGGTTATG
AIG1	CAATGGCAGAGATGATGGAG	TGCTCAAAGAGCTTCTCCTG
PR1	ACACGTGCAATGGAGTTTGTGG	TTGGCACATCCGAGTCTCACTG

Table 2. Continued

RT-PCR primers

ACTIN	GGCGATGAAGCTCAATCCAAAC G	GGTCACGACCAGCAAGATCAAGACG
NDR1	CGGGATCCATGAATAATCAAAAT GAAGACAC	GAAGGCCTACGAATAGCAAAGAATA CGAG
RAR1	GAAGATCTCCATGGAAGTAGGAT CTGCAACG	GAAGGCCTGACCGCCGGATCAGGG CTGC
RIN4	CGGGATCCATGGCACGTTCGAA TGTACC	TCCCCCGGGTTTTCCTCCAAAGCCA AAGCAGC
RPM1	GAAGATCTCCATGGCTTCGGCTA CTGTTG	GAAGGCCTAGATGAGAGGCTCACAT AG
RPS2	GCTAGTGAAGTTCTGACTAG	AACTGACAACACTGATGCTC
SGT1b	CATGCCATGGCCAAGGAATTAG CAGAG	GAAGGCCTATACTCCCACTTCTTGA GCTC
UBQ10	AGATCCAGGACAAGGAAGGTAT TC	CGCAGGACCAAGTGAAGAGTAG

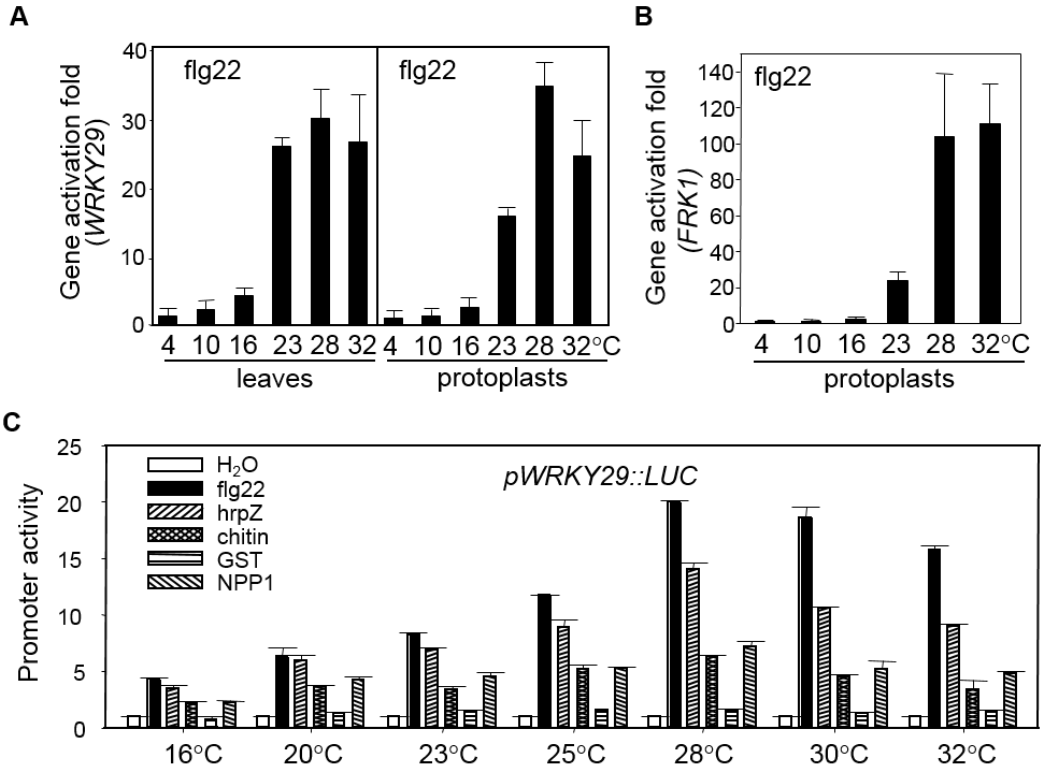

Figure 3.1 Elevated temperatures promote PTI responses. (A) flg22-induced WRKY29 activation in *Arabidopsis* leaves and protoplasts at different temperatures. Leaves or protoplasts from 4-week-old plants were treated with H2O or 100 nM flg22 for 3 h for RNA isolation and real-time RT-PCR (qRT-PCR) analysis. The expression of WRKY29 was normalized to the expression of UBQ10. (B) flg22-induced FRK1 activation in *Arabidopsis* protoplasts at different temperatures. Protoplasts from 4-week-old plants were treated with H2O or 100 nM flg22 for 3 h for RNA isolation and qRT-PCR analysis. The expression of FRK1 was normalized to the expression of UBQ10. The gene activation fold is presented as the ratio of flg22 treatment to H2O treatment with the mean±s.e.m. (n=3) from three independent biological replicates. (C) Activation of pWRKY29::LUC by different MAMPs at different temperatures. The protoplasts were transfected with pWRKY29::LUC and pUBQ::GUS as an internal control and treated with 10 nM flg22, 10 nM HrpZ, 50 μg ml^{-1} chitin, or 20 nM NPP1 for 3 h at the indicated temperatures. GST is the control for NPP1. The promoter activity was shown as the ratio of relative luciferase activity to GUS activity. The data are shown as mean ± s.e.m. (n=3) from three independent biological replicates. The above experiments were repeated three times with similar results. Primers were listed in Table 2.

Results

Elevated temperatures promote PTI responses

To monitor the specific immune responses at different ambient temperatures, we first tested the impact of different temperatures on PTI responses. Elicitation of PTI in *Arabidopsis* is accompanied by profound immune gene transcriptional reprogramming. The PTI marker genes *WRKY29* and *FRK1* were preferentially activated at the elevated ambient temperatures between 23°C and 32°C in response to flg22 (a 22-amino acid peptide of bacterial flagellin) in *Arabidopsis* leaves or protoplasts (Figure 3.1A and 3.1B). The optimal temperature for *WRKY29* and *FRK1* activation by flg22 was around 28°C. The activation was dramatically reduced when the temperature was below 16°C. Plants perceive a variety of MAMPs with different receptors. The similar temperature preference was observed for the activation of *pWRKY29::LUC* (the *WRKY29* promoter fused with luciferase reporter) by other MAMPs, including bacterial harpin Z (HrpZ), fungal chitin and oomycete necrosis-inducing *Phytophthora* protein 1 (NPP1) (Figure 3.1C). Perception of different MAMPs elicits convergent early signaling events, including MAPK activation. The MAPK activation in seedlings treated with flg22 became gradually pronounced with the increased ambient temperatures (Figure 3.2A). Apparently, the activation of MAPKs by flg22 at 28°C or 23°C occurred faster and stronger than that at 16°C. It has also been observed that flg22-induced FLS2-BAK1 receptor complex was not formed at 4°C (Chinchilla et al., 2007). Consistently, flg22-induced phosphorylation of BIK1 was largely reduced at 16°C but increased at 28°C (Figure 3.2B). It is unlikely that

the enhanced kinase activation results from elevated protein synthesis at higher temperatures since the samples were incubated at different temperatures for a relatively short time period (from 5 to 45 min). Thus, plants exhibit preference to operate PTI responses at a relatively high ambient temperature above 23°C. The *in vitro* bacterial growth assay indicates that bacterium *P. syringae* pv. *tomato* DC3000 (*Pst*) multiplies more vigorously at the elevated ambient temperatures above 23°C than at temperatures below 16°C. The increased bacterial growth rate at the elevated ambient temperatures likely leads to the production of more MAMPs.

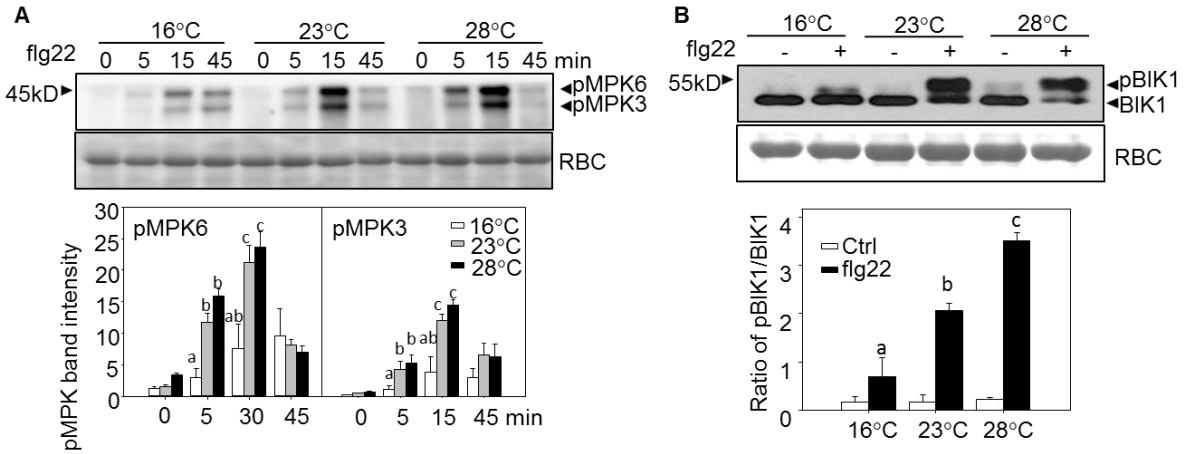

Figure 3.2 Elevated temperatures promote early PTI signaling. (A) flg22-induced MAPK activation at different temperatures. Ten-day old WT seedlings were treated with 100 nM flg22 at different temperatures for indicated time. MAPK activation was detected with an α-pERK antibody and Coomassie Brilliant Blue staining of Rubisco (RBC) protein is shown for equal loading control. (B) flg22-induced BIK1 phosphorylation in protoplasts at different temperatures. The band intensity of pMPK3, pMPK6, BIK1 and pBIK1 was quantified by the Image J software with mean ± s.e.m. (n=3) from three independent biological replicates. Bars without a common letter ("a", "b" and "c") are significantly different ($p<0.05$) at by One-way ANOVA followed by post hoc Tukey test for individual time points with SPSS software.

Elevated temperatures inhibit ETI responses

Our finding is surprising since it is generally believed that plant defense responses are inhibited at moderately elevated temperatures (Y. Wang, Bao, Zhu, & Hua, 2009). We further determined the temperature regulation of ETI responses triggered by the *P. syringae* effector AvrRpt2. To avoid the complication of bacterial physiology, multiplication and effector secretion/delivery at different temperatures, we examined the immune responses in dexamethasone (Dex)-inducible AvrRpt2 transgenic plants (McNellis et al., 1998). Treatment with Dex induced the expression of the *AvrRpt2* gene in *Dex-AvrRpt2* plants. The AvrRpt2 initiates the ETI signaling that then induces the expression of WRKY46 (X. Gao et al., 2013). Interestingly, the activation of *WRKY46* by AvrRpt2 was also temperature sensitive (Figure 3.3A). However, a distinct temperature preference was observed for ETI compared to PTI. The *WRKY46* activation was detectable when temperature was as low as 4°C, peaked at 16°C, but was significantly attenuated when the temperature was above 28°C (Fig. 3.3A). A similar *WRKY46* induction pattern was observed when AvrRpt2 was expressed in protoplasts at different temperatures (Figure 3.3A). We also detected the temperature modulation of *WRKY46* activation mediated by NLR protein RPM1 in response to *P. syringae* effector AvrRpm1 or AvrB (Figure 3.3B). The optimal activation of *WRKY46* by AvrRpm1 or AvrB was also observed at 16°C, and the elevated temperatures suppressed *WRKY46* activation (Fig. 3.3B). In addition, the AvrRpt2-mediated cell death in *Dex-AvrRpt2* plants was

significantly reduced at 28°C and was almost completely abolished at 32°C (Figure 3.3C). Interestingly, the cell death was clearly observed even at 4°C. The *avrRpt2* gene expressed at similar level after Dex treatment at different temperatures (Figure 3.3C). The reduced activity of AvrRpt2, AvrRpm1 and AvrB at the elevated ambient temperatures was not due to the reduced protein expression (Figure 3.4A). The data indicate that elevated temperatures could suppress *Arabidopsis* NLR protein RPM1 and RPS2-mediated ETI signaling. This observation is consistent with that the disease resistance and HR induced by *Pst* carrying *avrRpt2* or *avrRpm1* were reduced at 28°C compared with that at 22°C (Wang et al., 2009).

Elevated temperature does not affect NLR and signaling gene expression

The compromised NLR immune responses at the elevated temperatures could be a result of reduced transcript/protein level of NLRs or other components in NLR signaling (Bieri et al., 2004). We compared the RPS2 protein level in *pRPS2::RPS2-HA* transgenic plants at 23°C and 32°C. The RPS2 protein level did not differ significantly in plants incubated at 32°C for 9 hr compared with that at 23°C (Figure 3.4B). Similarly, the transcripts of *RPM1, RPS2, RIN4*, *RAR1, NDR1* and *SGT1b* were comparable in plants incubated at 23°C and 32°C (Figure 3.4C). Thus, the short-term treatment with the elevated ambient temperatures unlikely changed NLR protein stability, signaling component transcripts or other plant physiology. AvrRpt2 degrades *Arabidopsis* RIN4 protein to activate RPS2 signaling (Axtell & Staskawicz, 2003; Mackey et al., 2003). Apparently, the AvrRpt2-mediated RIN4 degradation still occurred at 28°C and 32°C,

although the HR was significantly blocked at these elevated temperatures (Figure 3.4D). Similarly, AvrRpm1-mediated RIN4 phosphorylation as shown with a mobility shift seems not affected by the elevated temperature (Figure 3.4E). The data suggest that the temperature operation of ETI responses occurs independent or downstream of RIN4 modification.

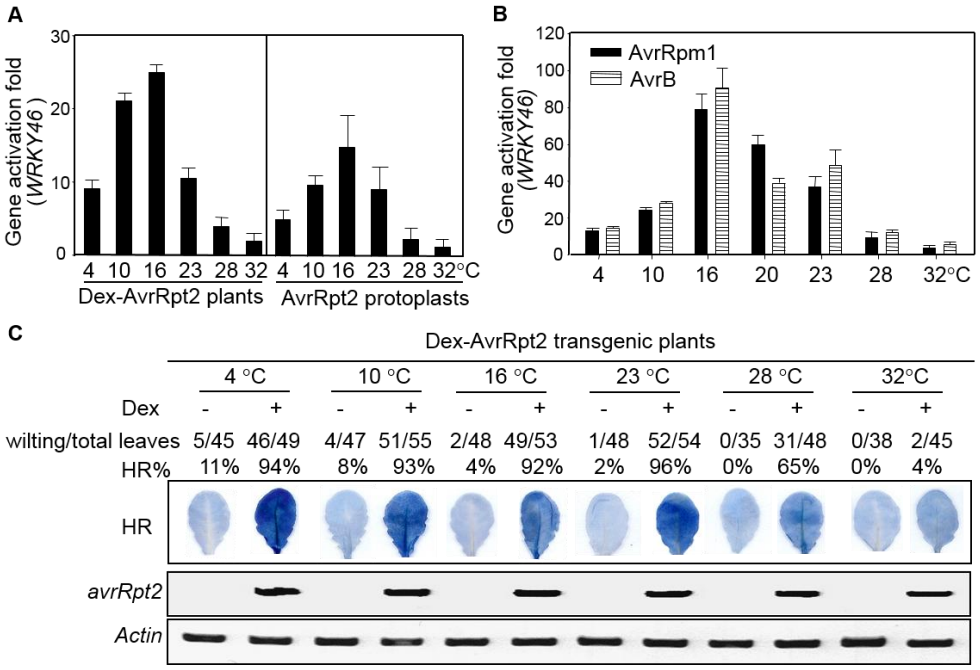

Figure 3.3 Elevated temperatures inhibit ETI responses. (A) Activation of *WRKY46* by AvrRpt2 at different temperatures. Four-week-old *Dex-AvrRpt2* plants were hand-inoculated with H_2O or 10 μM Dex, or the protoplasts were transfected with AvrRpt2 or a vector control, and incubated at different temperatures for 6 hr before sample collection for RNA isolation. The gene activation fold is presented as the ratio of *AvrRpt2* expression to controls with the mean ± SE (n=3) from three independent biological replicates. (B) Activation of *WRKY46* by AvrRpm1 or AvrB at different temperatures. The protoplasts were transfected with *AvrRpm1*, *AvrB* or a vector control, and incubated at different temperatures for 6 hr before sample collection for RNA isolation. (C) Cell death in *DEX-avrRpt2* transgenic plants at different temperatures. The *DEX-avrRpt2* transgenic plants were hand-inoculated with H_2O or 10 μM Dex, and incubated at different temperatures. The cell death was recorded 24 hpi for plants incubated at 16, 23, 28 and 32°C, 40 hpi for

plants at 10°C, and 48 hpi for plants at 4°C. The cell death was shown by Trypan blue staining and % indicates the percentage of wilting leaves of total inoculated leaves. The expression of *avrRpt2* after DEX treatment is shown. Actin is the control for RT-PCR.

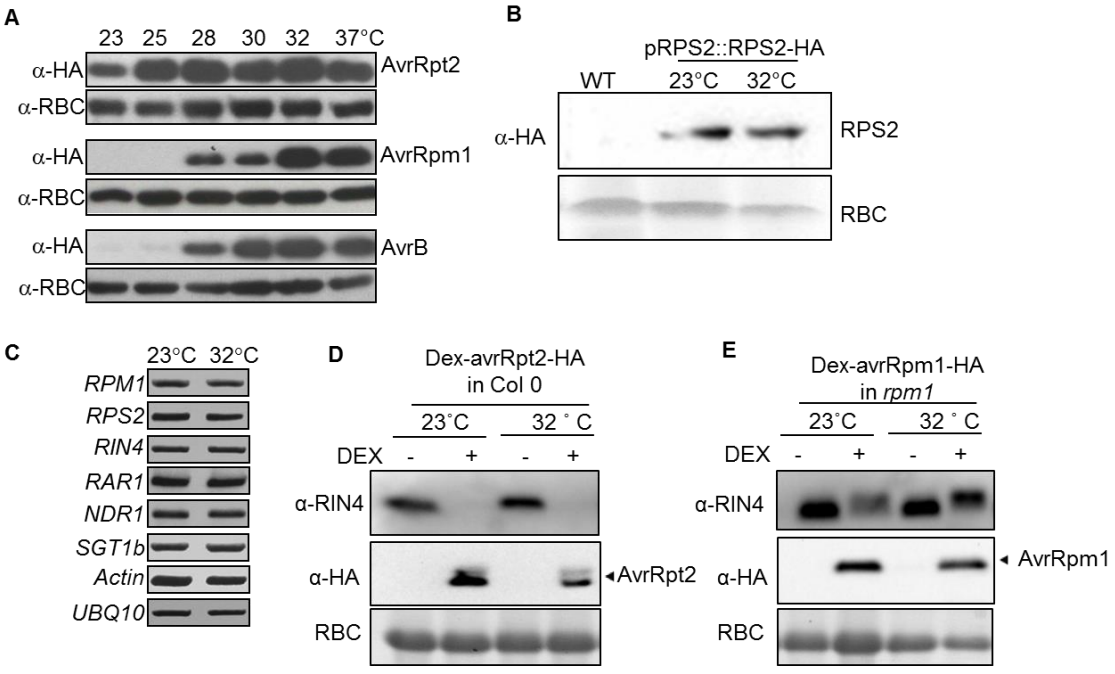

Figure 3.4. Elevated temperatures do not suppress expression of bacterial effector genes, plant resistance and signaling genes. (A) Expression of effector proteins at different temperatures. The protoplasts were transfected with *AvrRpt2*, *AvrRpm1*, or *AvrB*, and incubated at different temperatures for 6 hr before sample collection for Western blot with an α-HA antibody. Western blot with an α-RBC (Rubisco) antibody is shown as a loading control. (B) RPS2 protein level at 23°C and 32°C. The *pRPS2::RPS2-HA* plants were incubated at 23°C and 32°C for 9 hr before sample collection for Western blot with an α-HA antibody. (C) Expression of plant resistance and signaling genes at 23°C and 32°C by RT-PCR analysis. The plants were incubated 23°C and 32°C for 6 hr before sample collection for RNA isolation. AvrRpt2-mediated RIN4 degradation (D) and AvrRpm1-mediated RIN4 phosphorylation (E) at different temperatures. Dex-AvrRpt2-HA (in Col-0 background) or Dex-AvrRpm1-HA transgenic plants (in *rpm1* background*)* were pre-warmed at different temperatures for 1 hr and then infiltrated with 10μM Dex or H_2O for 8 hr. Immunoblot was performed with an α-RIN4 or α-HA antibody. Staining of RBC shows equal loading.

Enhanced PTI responses in arp6-10 and hta9hta11 mutant plants

Recent research has identified some important players in response to ambient temperature changes in plants (Samach & Wigge, 2005). In particular, alternative histone H2A.Z nucleosomes are essential for *Arabidopsis* to precisely perceive ambient temperature, and may function as an evolutionarily conserved thermosensor to regulate the ambient temperature transcriptome (Kumar & Wigge, 2010). The *Arabidopsis* mutants deficient in incorporating H2A.Z into nucleosomes, such as *arp6* and *hta9hta11,* phenocopy plants grown at the elevated ambient temperature and possess constitutive warm temperature transcriptome (Kumar & Wigge, 2010). At higher temperature, H2A.Z nucleosome occupancy declines, which leads to the expression of warm temperature responsive genes. Consistently, in the absence of H2A.Z deposition, such as *arp6* and *hta9hta11* mutants, plants display a constitutive warm temperature responses (Kumar & Wigge, 2010).We therefore determined the PTI and ETI responses in *arp6* and *hta9hta11* mutants. We first compared the flg22-induced MAPK activation in *hta9hta11* and *arp6* mutants at 23°C. Obviously, the activation of MAPKs by flg22 was stronger in both *hta9hta11* and *arp6* mutants than that in wild-type (WT) plant seedlings, in particular 15 min after treatment (Figure 3.5A). Many PTI marker genes were identified from previous microarray experiments (He et al., 2006). The induction of the marker gene *FRK1* and *At2g17740* by flg22 treatment was also enhanced in *hta9hta11* and/or *arp6* mutants compared to that in WT seedlings (Figure 3.5B). Consistent with the enhanced PTI

responses, it has been reported that *hta9hta11* mutant displayed enhanced resistance to *Pst* infection (March-Diaz et al., 2008).

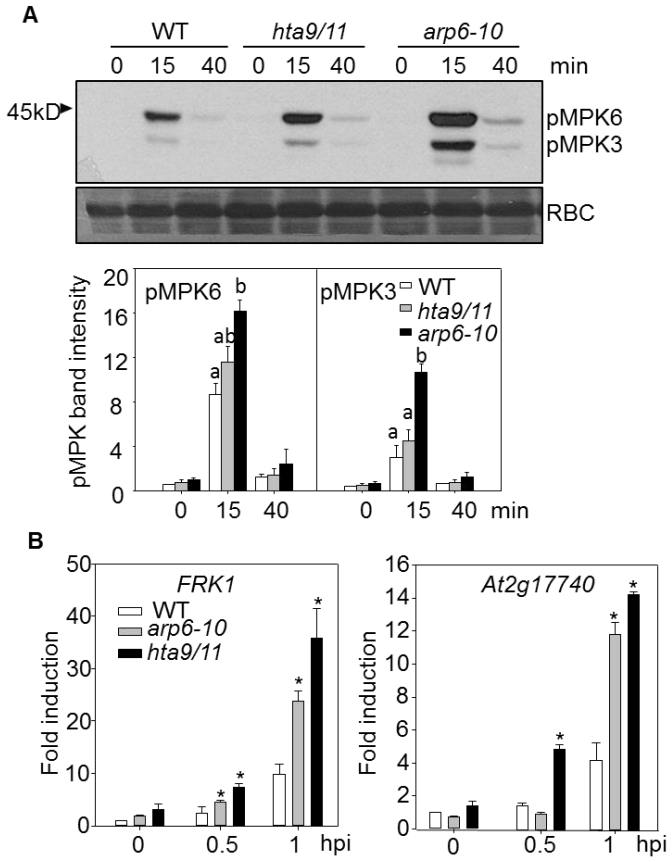

Figure 3.5 Enhanced PTI responses in *arp6-10* and *hta9hta11* mutant plants. (A) flg22-induced MAPK activation in WT and mutants. Ten-day old seedlings were treated with 100 nM flg22 at room temperature for indicated time. MAPK activation was detected with an α-pERK antibody. The band intensity of pMPK3, pMPK6 was quantified by the Image J software with mean ± s.e.m. (n=3) from three independent biological replicates. Bars without a common letter ("a" and "b") are significantly different ($p<0.05$) at by One-way ANOVA followed by post hoc Tukey test for individual time points with SPSS software. (B) flg22-induced PTI marker gene expression. 10-day-old seedlings of WT and mutants were treated with 100 nM flg22 for 0.5 or 1 hr. The gene expression of *FRK1* and *At2g17740* was detected by q RT-PCR and normalized to the expression of *UBQ10*. The data are shown as the mean ± s.e.m. from three independent biological replicates. * indicates a significant difference with $p<0.05$ analyzed with SPSS software with one-way ANOVA analysis (SPSS Inc., Chicago) when compared with data from WT plants. Primers were listed in Table 2.

Reduced ETI responses in arp6-10 and hta9hta11 mutant plants

In contrast to the enhanced PTI responses, the ETI responses were reduced in the *hta9hta11* and *arp6* mutants. The inoculation of *Pst avrRpt2* or *avrRpm1* at a relatively high inoculum elicits an HR in WT *Arabidopsis* plants (Figure 3.6 A&B). The leaves inoculated with *Pst avrRpt2* show tissue collapse at about 12~24 hours post-inoculation (*hpi*), and the *Pst avrRpm1*-inoculated leaves show collapse at about 4~12 *hpi* . The progression of *Pst avrRpt2* and *avrRpm1*-triggered HR was slower in the *hta9hta11* and *arp6* mutants than that in WT plants (Figure 3.6A & 6B). We also quantified HR using an electrolyte leakage assay. Consistently, compared to WT plants, *hta9hta11* and *arp6* mutants showed a compromised increase in conductance, due to the release of electrolytes during cell death upon *Pst avrRpt2* or *avrRpm1* infection (Figure 3.6C & 6D). The *in planta* bacterial multiplication of *Pst avrRpt2* increased about 10 fold in the *hta9hta11* and *arp6* mutants compared to that in WT plants (Figure 3.7A). The bacterial multiplication of *Pst avrRpm1* increased about 5 fold in the *arp6* mutant compared to that in WT plants (Figure 3.7A). The *Pst avrRpt2* or *avrRpm1* infection induces expression of several defense-related genes, such as *AIG1* and *PR1*. The induction of *AIG1* and *PR1* by *Pst avrRpt2* or *avrRpm1* was significantly lower in *hta9hta11* and *arp6* mutants than that in WT plants (Figure 3.7B). The data are consistent with the differential operation of two branches of plant innate immune signaling at different temperatures.

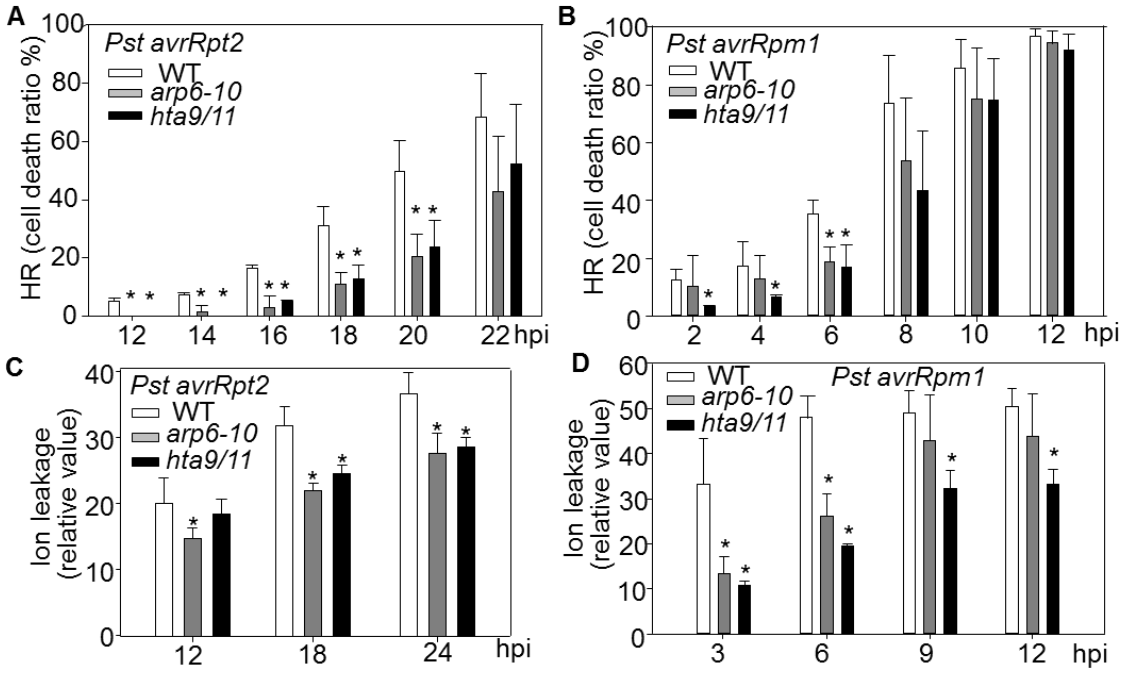

Figure 3.6 Reduced ETI cell death in *arp6-10* and *hta9hta11* mutant plants. Compromised HR triggered by *Pst avrRpt2* (A) and *avrRpm1* (B) in *arp6-10* and *hta9/11* mutant plants. Four-week-old WT and mutant plants were hand-inoculated with bacteria at a concentration of 1 x 10^8 cfu/ml. HR was examined by counting the percentage of wilting leaves of total inoculated leaves (>20) at different time points after inoculation. Electrolyte leakage induced by *Pst avrRpt2* (C) and *avrRpm1* (D) was reduced in *arp6-10* and *hta9/11* mutant plants. Five leaf discs were excised from 4-week-old plants hand-inoculated with bacteria at 1 x 10^8 cfu/ml for each sample at each time point with three replicates. The data are shown as the mean ± s.e.m. (n=3) from three independent biological replicates and the asterisk (*) indicates a significant difference with $p<0.05$ analyzed with SPSS software with one-way ANOVA analysis (SPSS Inc., Chicago) when compared with data from WT plants.

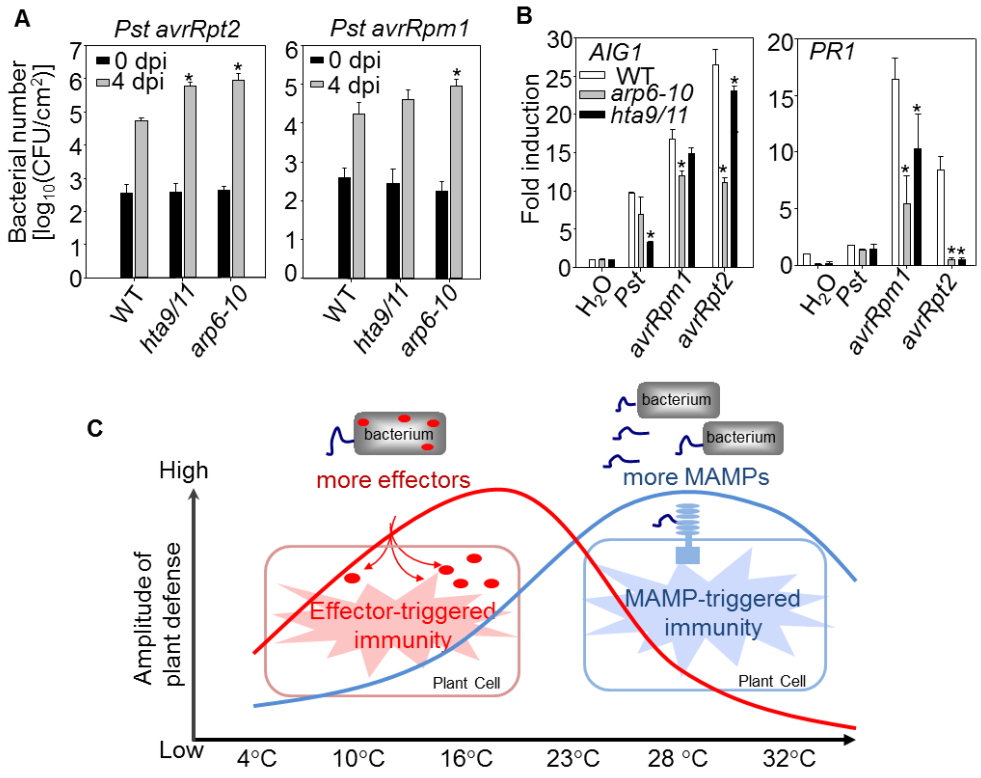

Figure 3.7 Compromised ETI-mediated restriction of bacterial growth and defense gene activation in *arp6-10* and *hta9hta11* mutant plants. (A) Bacterial growth assay. Four-week-old plants were hand-inoculated with *Pst avrRpm1* or *avrRpt2* at 5 x 10^5 cfu/ml. The bacterial growth was measured 0 days post-inoculation (dpi) or 4 dpi. (B) ETI marker gene expression. Four-week-old plants were hand-inoculated with bacteria at 1 x 10^7 cfu/ml, and RNA was collected 6 hpi for qRT-PCR analysis. The expression of *AIG1* and *PR1* was normalized to the expression of *UBQ10*. The data are shown as the mean ± s.e.m. (n=3) from three independent biological replicates and the asterisk (*) indicates a significant difference with $p<0.05$ analyzed with SPSS software with one-way ANOVA analysis (SPSS Inc., Chicago) when compared with data from WT plants. (C) A model of temperature operation of distinct plant innate immune responses. At low ambient temperatures, bacteria secrete a large suite of virulence effectors to promote pathogenicity, which in turn stimulates plants to co-evolve and preferentially activate ETI signaling. At the elevated temperatures, bacteria multiply vigorously and produce increased amount of MAMPs, which stimulate plants to switch to PTI signaling. Ambient temperature fluctuation likely drives the dynamic co-evolution of bacterial pathogenesis and host immunity.

Discussion

Microbes and hosts have co-evolved dynamically in their arms race for fitness and survival. Environmental factors often influence the physiological responses on both sides and have profound impacts on microbial pathogenesis and host immunity. In this study, we performed quantitative assays for immune responses based on the activation of specific marker genes and found differential temperature preferences for the activation of two branches of plant innate immunity. Bacterial effector-triggered immune responses are preferentially activated at relatively lower ambient temperatures which are suitable for effector secretion, and suppressed at the elevated ambient temperatures. The inhibition of ETI responses was not caused by the reduced expression of effectors, corresponding NLR receptors or known signaling components. In contrast, PAMP-triggered immune responses are preferentially activated at the elevated ambient temperatures which are optimal for bacterial growth, and suppressed at lower temperatures. Consistently, the immune responses of *arp6* and *hta9hta11* mutant plants, which are deficient in temperature sensing and phenocopy high temperature-grown plants, mimic the responses of plants at the elevated temperatures with enhanced PTI signaling and yet reduced ETI signaling. Plant PTI signaling is initiated via cell-surface RLKs whereas ETI signaling is mediated through intracellular NLR immune receptors. Although the precise mechanisms of how temperature sensing and signaling modulate the distinct plant immune responses are waiting to be elucidated, the differential temperature preferences of PTI and ETI responses suggests the distinct early signaling events downstream of cell surface RLKs

and intracellular NLR immune sensors. Our findings may have broad implication for agricultural practices to optimize plant immunity by considering the temperature-based defense strategies.

Plant NLR proteins differ in the N-terminal domain and were further divided into CC (coiled-coil)-domain-containing and TIR (Toll-interleukin-1 receptor)-domain containing classes (DeYoung & Innes, 2006; Maekawa et al., 2011). Growing evidence suggests the signaling activation in distinct subcellular compartments in TIR-NLR- and CC-NLR-mediated immunity (Heidrich et al., 2012). In several cases, TIR-NLR-mediated immunity is temperature sensitive (Whitham, Dinesh-Kumar et al. 1994, Yang and Hua 2004, Burch-Smith, Schiff et al. 2007, Mang et al. 2012). For instance, the tobacco mosaic virus resistance *N* gene and *Arabidopsis SNC1* gene-mediated responses are compromised at the elevated ambient temperatures above 28°C (Whitham et al., 1994; Yang & Hua, 2004). Interestingly, suppressor screens and targeted mutagenesis suggest that SNC1 itself is a temperature-sensitive component of plant immune responses (Zhu et al. 2010). Several TIR-NLR immune receptors function in nucleus (Burch-Smith et al., 2007; Cheng et al., 2009; Heidrich et al., 2011; Mang et al., 2012), whereas RPM1 and RPS2, the CC-NLR immune receptors, localize to plasma membrane to initiate ETI signaling (Axtell & Staskawicz, 2003; Gao et al., 2011). Our study indicates that RPM1 and RPS2-mediated responses are also largely compromised at temperatures above 28°C. Our data suggests NBS-LRR gene expression or protein accumulation was not affected by ambient temperature fluctuation, but we cannot rule out the qualitative changes under different

temperatures such as subcellular localization of R protein. Thus, both CC-NLR and TIR-NLR signaling pathways are modulated by ambient temperatures.

Unexpectedly, we found that cell surface-resident RLK-mediated PTI signalling is also temperature sensitive with a pattern distinct from ETI signalling. In contrast to gradually compromised ETI responses, PTI responses become incrementally active with the elevated ambient temperatures (Figure 3.7C). The differential temperature preference for the optimal operation of PTI and ETI signaling reconciles an enigmatic observation that the elevated temperatures inhibit bacterial effector secretion and yet promote bacterial proliferation (Smirnova et al., 2001; van Dijk et al., 1999). Accordingly, plants have evolved combating mechanisms to maximize the PTI responses and turn down specific NLR-mediated responses to cope with a broad spectrum of microbe invasions at the elevated temperatures. At low ambient temperatures, bacteria secrete a large suite of virulence effectors to promote pathogenicity (van Dijk et al., 1999), which in turn stimulates plants to co-evolve and preferentially activate ETI signaling (Figure 3.7C). Our results suggest that daily, seasonal or even geographical ambient temperature fluctuations drives the dynamic co-evolution of bacterial pathogenesis and host immunity, and plants integrate ambient temperature sensing to regulate two distinct branches of innate immunity mediated by cell surface RLK and intracellular NLR immune sensors.

Arabidopsis arp6 and *hta9hta11* mutants are deficient in incorporating histone H2A.Z into nucleosomes (Kumar & Wigge, 2010). ARP6 encodes a subunit of the evolutionarily conserved SWR1 complex that is necessary for inserting the alternative histone H2A.Z encoded by *HTA* gene family members into nucleosomes in place of H2A

(Kumar & Wigge, 2010; March-Diaz et al., 2008). H2A.Z-containing nucleosomes wrap DNA more tightly than canonical H2A nucleosomes and can modulate transcription in a temperature-dependent manner. It will be interesting to test whether *arp6* and *hta9hta11* mutants could suppress the temperature-dependent cell death in *snc1-1*, *mekk1* and *mpk4* mutants (Gao et al., 2008; Yang & Hua, 2004). Notably, the *hta9hta11* mutant also displayed constitutive expression of certain defense-related genes, spontaneous cell death and increased resistance to *Pst* infections, suggesting a link between H2A.Z-regulated gene expression and plant immunity (March-Diaz et al., 2008). Consistent with this observation, we showed that *arp6* and *hta9hta11* mutants have enhanced flg22-mediated responses. However, the ETI responses are suppressed in *arp6* and *hta9hta11* mutants, suggesting the opposite role of H2A.Z-containing nucleosomes in modulating PTI and ETI responses. Future study will uncover the molecular link between H2A.Z-mediated temperature perception and specific responses in ETI and PTI signaling.

REFERENCES

Agrios, G. N. (2005). *Plant pathology* (5th ed.). Burlington, MA: Elsevier Academic Press.

Albrecht, C., Boutrot, F., Segonzac, C., Schwessinger, B., Gimenez-Ibanez, S., Chinchilla, D., . . . Zipfel, C. (2012). Brassinosteroids inhibit pathogen-associated molecular pattern–triggered immune signaling independent of the receptor kinase BAK1. *Proc. Natl Acad. Sci. USA, 109*(1), 303-308.

Alcazar, R., & Parker, J. E. (2011). The impact of temperature on balancing immune responsiveness and growth in Arabidopsis. *Trends Plant Sci, 16*(12), 666-675.

Archambault, J., Chambers, R. S., Kobor, M. S., Ho, Y., Cartier, M., Bolotin, D., . . . Greenblatt, J. (1997). An essential component of a C-terminal domain phosphatase that interacts with transcription factor IIF in Saccharomyces cerevisiae. *Proc. Natl Acad. Sci. USA, 94*(26), 14300-14305.

Asai, T., Tena, G., Plotnikova, J., Willmann, M. R., Chiu, W.-L., Gomez-Gomez, L., . . . Sheen, J. (2002). MAP kinase signalling cascade in Arabidopsis innate immunity. *Nature, 415*(6875), 977-983.

Axtell, M. J., & Staskawicz, B. J. (2003). Initiation of RPS2-specified disease resistance in Arabidopsis is coupled to the AvrRpt2-directed elimination of RIN4. *Cell, 112*, 369-377.

Bartkowiak, B., Liu, P., Phatnani, H. P., Fuda, N. J., Cooper, J. J., Price, D. H., . . . Greenleaf, A. L. (2010). CDK12 is a transcription elongation-associated CTD kinase, the metazoan ortholog of yeast Ctk1. *Genes Dev, 24*(20), 2303-2316.

Bataille, A. R., Jeronimo, C., Jacques, P. E., Laramee, L., Fortin, M. E., Forest, A., . . . Robert, F. (2012). A universal RNA polymerase II CTD cycle is orchestrated by complex interplays between kinase, phosphatase, and isomerase enzymes along genes. *Mol Cell, 45*(2), 158-170.

Belkhadir, Y., Jaillais, Y., Epple, P., Balsemão-Pires, E., Dangl, J. L., & Chory, J. (2012). Brassinosteroids modulate the efficiency of plant immune responses to microbe-associated molecular patterns. *Proc. Natl Acad. Sci. USA, 109*(1), 297-302.

Bent, A. F., Kunkel, B. N., Dahlbeck, D., Brown, K. L., Schmidt, R., Giraudat, J., . . . Staskawicz, B. J. (1994). RPS2 of Arabidopsis thaliana: a leucine-rich repeat class of plant disease resistance genes. *Science, 265*(5180), 1856-1860.

Bethke, G., Pecher, P., Eschen-Lippold, L., Tsuda, K., Katagiri, F., Glazebrook, J., . . . Lee, J. (2012). Activation of the Arabidopsis thaliana mitogen-activated protein kinase MPK11 by the flagellin-derived elicitor peptide, flg22. *Mol Plant Microbe Interact, 25*(4), 471-480.

Bhattacharjee, S., Halane, M. K., Kim, S. H., & Gassmann, W. (2011). Pathogen effectors target Arabidopsis EDS1 and alter its interactions with immune regulators. *Science, 334*(6061), 1405-1408.

Bieri, S., Mauch, S., Shen, Q. H., Peart, J., Devoto, A., Casais, C., . . . Schulze-Lefert, P. (2004). RAR1 positively controls steady state levels of barley MLA resistance proteins and enables sufficient MLA6 accumulation for effective resistance. *Plant Cell, 16*(12), 3480-3495.

Block, A., & Alfano, J. R. (2011). Plant targets for Pseudomonas syringae type III effectors: virulence targets or guarded decoys? *Curr Opin Microbiol, 14*(1), 39-46.

Boller, T., & Felix, G. (2009). A renaissance of elicitors: perception of microbe-associated molecular patterns and danger signals by pattern-recognition receptors. *Annu Rev Plant Biol, 60*, 379-406.

Boudsocq, M., Willmann, M. R., McCormack, M., Lee, H., Shan, L., He, P., . . . Sheen, J. (2010). Differential innate immune signalling via Ca2+ sensor protein kinases. *Nature, 464*(7287), 418-422.

Boudsocq, M., Willmann, M. R., McCormack, M., Lee, H., Shan, L., He, P., . . . Sheen, J. (2010). Differential innate immune signalling via Ca(2+) sensor protein kinases. *Nature, 464*(7287), 418-422.

Buratowski, S. (2009). Progression through the RNA polymerase II CTD cycle. *Mol Cell, 36*(4), 541-546.

Burch-Smith, T. M., Schiff, M., Caplan, J. L., Tsao, J., Czymmek, K., & Dinesh-Kumar, S. P. (2007). A novel role for the TIR domain in association with pathogen-derived elicitors. *PLoS Biol, 5*(3), e68.

Chapman, R. D., Heidemann, M., Hintermair, C., & Eick, D. (2008). Molecular evolution of the RNA polymerase II CTD. *Trends Genet, 24*(6), 289-296.

Cheng, Y. T., Germain, H., Wiermer, M., Bi, D., Xu, F., Garcia, A. V., . . . Li, X. (2009). Nuclear pore complex component MOS7/Nup88 is required for innate immunity

and nuclear accumulation of defense regulators in Arabidopsis. *Plant Cell, 21*(8), 2503-2516.

Chinchilla, D., Zipfel, C., Robatzek, S., Kemmerling, B., Nurnberger, T., Jones, J. D., . . . Boller, T. (2007). A flagellin-induced complex of the receptor FLS2 and BAK1 initiates plant defence. *Nature, 448*(7152), 497-500.

Cui, X. F., Fan, B. F., Scholz, J., & Chen, Z. X. (2007). Roles of Arabidopsis cyclin-dependent kinase C complexes in cauliflower mosaic virus infection, plant growth, and development. *Plant Cell, 19*(4), 1388-1402.

DeYoung, B. J., & Innes, R. W. (2006). Plant NBS-LRR proteins in pathogen sensing and host defense. *Nat Immunol, 7*(12), 1243-1249.

Dietrich, M. A., Prenger, J. P., & Guilfoyle, T. J. (1990). Analysis of the genes encoding the largest subunit of RNA polymerase II in Arabidopsis and soybean. *Plant Mol Biol, 15*(2), 207-223.

Dodds, P. N., & Rathjen, J. P. (2010). Plant immunity: towards an integrated view of plant-pathogen interactions. *Nat Rev Genet, 11*(8), 539-548.

Dong, C., Davis, R. J., & Flavell, R. A. (2002). MAP kinases in the immune response. *Annual Review of Immunology, 20*(1), 55-72.

Egloff, S., & Murphy, S. (2008). Cracking the RNA polymerase II CTD code. *Trends Genet, 24*(6), 280-288.

Esnault, C., Ghavi-Helm, Y., Brun, S., Soutourina, J., Van Berkum, N., Boschiero, C., . . . Werner, M. (2008). Mediator-dependent recruitment of TFIIH modules in preinitiation complex. *Mol Cell, 31*(3), 337-346.

Feng, F., Yang, F., Rong, W., Wu, X., Zhang, J., Chen, S., . . . Zhou, J.-M. (2012). A Xanthomonas uridine 5 [prime]-monophosphate transferase inhibits plant immune kinases. *Nature, 485*(7396), 114-118.

Feng, Y., Kang, J. S., Kim, S., Yun, D. J., Lee, S. Y., Bahk, J. D., & Koiwa, H. (2010). Arabidopsis SCP1-like small phosphatases differentially dephosphorylate RNA polymerase II C-terminal domain. *Biochem Biophys Res Commun, 397*(2), 355-360.

Flor, H. H. (1942). Inheritance of pathogenicity in Melampsora lini. *Phytopathology, 32*, 16.

Gao, M., Liu, J., Bi, D., Zhang, Z., Cheng, F., Chen, S., & Zhang, Y. (2008). MEKK1, MKK1/MKK2 and MPK4 function together in a mitogen-activated protein kinase cascade to regulate innate immunity in plants. *Cell Res, 18*(12), 1190-1198.

Gao, X., Chen, X., Lin, W., Chen, S., Lu, D., Niu, Y., . . . Sheen, J. (2013). Bifurcation of Arabidopsis NLR immune signaling via Ca2+-dependent protein kinases. *PLoS pathogens, 9*(1), e1003127.

Gao, Z., Chung, E. H., Eitas, T. K., & Dangl, J. L. (2011). Plant intracellular innate immune receptor Resistance to Pseudomonas syringae pv. maculicola 1 (RPM1) is activated at, and functions on, the plasma membrane. *Proc. Natl Acad. Sci. USA, 108*(18), 7619-7624.

Ghosh, A., Shuman, S., & Lima, C. D. (2008). The structure of Fcp1, an essential RNA polymerase II CTD phosphatase. *Mol Cell, 32*(4), 478-490.

Gomez-Gomez, L., & Boller, T. (2000). FLS2: an LRR receptor-like kinase involved in the perception of the bacterial elicitor flagellin in Arabidopsis. *Mol Cell, 5*(6), 1003-1011.

Gou, X., Yin, H., He, K., Du, J., Yi, J., Xu, S., . . . Li, J. (2012). Genetic evidence for an indispensable role of somatic embryogenesis receptor kinases in brassinosteroid signaling. *PLoS genetics, 8*(1), e1002452.

Grant, M. R., Godiard, L., Straube, E., Ashfield, T., Lewald, J., Sattler, A., . . . Dangl, J. L. (1995). Structure of the Arabidopsis RPM1 gene enabling dual specificity disease resistance. *Science, 269*(5225), 843-846.

Guo, Z., & Stiller, J. W. (2004). Comparative genomics of cyclin-dependent kinases suggest co-evolution of the RNAP II C-terminal domain and CTD-directed CDKs. *BMC Genomics, 5*, 69.

Hajheidari, M., Farrona, S., Huettel, B., Koncz, Z., & Koncz, C. (2012). CDKF;1 and CDKD Protein Kinases Regulate Phosphorylation of Serine Residues in the C-Terminal Domain of Arabidopsis RNA Polymerase II. *Plant Cell, 24*(4), 1626-1642.

Hausmann, S., & Shuman, S. (2002). Characterization of the CTD phosphatase Fcp1 from fission yeast. Preferential dephosphorylation of serine 2 versus serine 5. *J Biol Chem, 277*(24), 21213-21220.

Hausmann, S., & Shuman, S. (2003). Defining the active site of Schizosaccharomyces pombe C-terminal domain phosphatase Fcp1. *J Biol Chem, 278*(16), 13627-13632.

He, K., Gou, X., Yuan, T., Lin, H., Asami, T., Yoshida, S., . . . Li, J. (2007). BAK1 and BKK1 regulate brassinosteroid-dependent growth and brassinosteroid-independent cell-death pathways. *Current Biology, 17*(13), 1109-1115.

He, P., Shan, L., Lin, N. C., Martin, G. B., Kemmerling, B., Nurnberger, T., & Sheen, J. (2006). Specific bacterial suppressors of MAMP signaling upstream of MAPKKK in Arabidopsis innate immunity. *Cell, 125*(3), 563-575.

Heese, A., Hann, D. R., Gimenez-Ibanez, S., Jones, A. M., He, K., Li, J., . . . Rathjen, J. P. (2007). The receptor-like kinase SERK3/BAK1 is a central regulator of innate immunity in plants. *Proc. Natl Acad. Sci. USA, 104*(29), 12217-12222.

Heidrich, K., Blanvillain-Baufume, S., & Parker, J. E. (2012). Molecular and spatial constraints on NB-LRR receptor signaling. *Curr Opin Plant Biol, 15*(4), 385-391.

Heidrich, K., Wirthmueller, L., Tasset, C., Pouzet, C., Deslandes, L., & Parker, J. E. (2011). Arabidopsis EDS1 connects pathogen effector recognition to cell compartment-specific immune responses. *Science, 334*(6061), 1401-1404.

Ichimura, K., Casais, C., Peck, S. C., Shinozaki, K., & Shirasu, K. (2006). MEKK1 is required for MPK4 activation and regulates tissue-specific and temperature-dependent cell death in Arabidopsis. *J Biol Chem, 281*(48), 36969-36976.

Jeworutzki, E., Roelfsema, M. R., Anschutz, U., Krol, E., Elzenga, J. T., Felix, G., . . . Becker, D. (2010). Early signaling through the Arabidopsis pattern recognition receptors FLS2 and EFR involves Ca-associated opening of plasma membrane anion channels. *Plant J, 62*(3), 367-378.

Jia, Y., McAdams, S. A., Bryan, G. T., Hershey, H. P., & Valent, B. (2000). Direct interaction of resistance gene and avirulence gene products confers rice blast resistance. *The EMBO Journal, 19*(15), 4004-4014.

Jin, Y. M., Jung, J., Jeon, H., Won, S. Y., Feng, Y., Kang, J. S., . . . Kim, M. (2011). AtCPL5, a novel Ser-2-specific RNA polymerase II C-terminal domain phosphatase, positively regulates ABA and drought responses in Arabidopsis. *New Phytol*. 190(1):57-74.

Kaku, H., Nishizawa, Y., Ishii-Minami, N., Akimoto-Tomiyama, C., Dohmae, N., Takio, K., . . . Shibuya, N. (2006). Plant cells recognize chitin fragments for defense

signaling through a plasma membrane receptor. *Proc. Natl Acad. Sci. USA, 103*(29), 11086-11091.

Kamenski, T., Heilmeier, S., Meinhart, A., & Cramer, P. (2004). Structure and mechanism of RNA polymerase II CTD phosphatases. *Mol Cell, 15*(3), 399-407.

Kimura, M., Suzuki, H., & Ishihama, A. (2002). Formation of a carboxy-terminal domain phosphatase (Fcp1)/TFIIF/RNA polymerase II (pol II) complex in Schizosaccharomyces pombe involves direct interaction between Fcp1 and the Rpb4 subunit of pol II. *Mol Cell Biol, 22*(5), 1577-1588.

Koiwa, H., Barb, A. W., Xiong, L., Li, F., McCully, M. G., Lee, B. H., . . . Hasegawa, P. M. (2002). C-terminal domain phosphatase-like family members (AtCPLs) differentially regulate Arabidopsis thaliana abiotic stress signaling, growth, and development. *Proc. Natl Acad. Sci. USA, 99*(16), 10893-10898.

Koiwa, H., Bressan, R. A., & Hasegawa, P. M. (2006). Identification of plant stress-responsive determinants in Arabidopsis by large-scale forward genetic screens. *J Exp Bot, 57*(5), 1119-1128.

Koiwa, H., Hausmann, S., Bang, W. Y., Ueda, A., Kondo, N., Hiraguri, A., . . . Shuman, S. (2004). Arabidopsis C-terminal domain phosphatase-like 1 and 2 are essential Ser-5-specific C-terminal domain phosphatases. *Proc. Natl Acad. Sci. USA, 101*(40), 14539-14544.

Kong, Q., Qu, N., Gao, M., Zhang, Z., Ding, X., Yang, F., . . . Li, X. (2012). The MEKK1-MKK1/MKK2-MPK4 Kinase Cascade Negatively Regulates Immunity Mediated by a Mitogen-Activated Protein Kinase Kinase Kinase in Arabidopsis. *Plant Cell, 24*(5), 2225-2236.

Konkel, M. E., & Tilly, K. (2000). Temperature-regulated expression of bacterial virulence genes. *Microbes Infect, 2*(2), 157-166.

Koressaar, T., & Remm, M. (2007). Enhancements and modifications of primer design program Primer3. *Bioinformatics, 23*(10), 1289-1291.

Kumar, S. V., & Wigge, P. A. (2010). H2A.Z-containing nucleosomes mediate the thermosensory response in Arabidopsis. *Cell, 140*(1), 136-147.

Lee, C. T., Zhong, L., Mace, T. A., & Repasky, E. A. (2012). Elevation in body temperature to fever range enhances and prolongs subsequent responsiveness of macrophages to endotoxin challenge. *PLoS One, 7*(1), e30077.

Lee, S. W., Han, S. W., Sririyanum, M., Park, C. J., Seo, Y. S., & Ronald, P. C. (2009). A type I-secreted, sulfated peptide triggers XA21-mediated innate immunity. *Science, 326*(5954), 850-853.

Lemaitre, B., Nicolas, E., Michaut, L., Reichhart, J. M., & Hoffmann, J. A. (1996). The dorsoventral regulatory gene cassette spatzle/Toll/cactus controls the potent antifungal response in Drosophila adults. *Cell, 86*(6), 973-983.

Liu, J., Elmore, J. M., Lin, Z.-J. D., & Coaker, G. (2011). A receptor-like cytoplasmic kinase phosphorylates the host target RIN4, leading to the activation of a plant innate immune receptor. *Cell Host & Microbe, 9*(2), 137-146.

Liu, Z., Wu, Y., Yang, F., Zhang, Y., Chen, S., Xie, Q., . . . Zhou, J.-M. (2013). BIK1 interacts with PEPRs to mediate ethylene-induced immunity. *Proc. Natl Acad. Sci. USA, 110*(15), 6205-6210.

Lu, D., Lin, W., Gao, X., Wu, S., Cheng, C., Avila, J., . . . Shan, L. (2011). Direct ubiquitination of pattern recognition receptor FLS2 attenuates plant innate immunity. *Science, 332*(6036), 1439-1442.

Lu, D., Wu, S., Gao, X., Zhang, Y., Shan, L., & He, P. (2010). A receptor-like cytoplasmic kinase, BIK1, associates with a flagellin receptor complex to initiate plant innate immunity. *Proc. Natl Acad. Sci. USA, 107*(1), 496-501.

Mackey, D., Belkhadir, Y., Alonso, J., Ecker, J., & Dangl, J. (2003). Arabidopsis RIN4 is a target of the type III virulence effector AvrRpt2 and modulates RPS2-mediated resistance. *Cell, 112*(3), 379-389.

Mackey, D., Holt 3rd, B., Wiig, A., & Dangl, J. (2002). RIN4 interacts with Pseudomonas syringae type III effector molecules and is required for RPM1-mediated resistance in Arabidopsis. *Cell, 108*(6), 743.

Maekawa, T., Kufer, T. A., & Schulze-Lefert, P. (2011). NLR functions in plant and animal immune systems: so far and yet so close. *Nat Immunol, 12*(9), 817-826.

Mang, H. G., Qian, W., Zhu, Y., Qian, J., Kang, H. G., Klessig, D. F., & Hua, J. (2012). Abscisic acid deficiency antagonizes high-temperature inhibition of disease resistance through enhancing nuclear accumulation of resistance proteins SNC1 and RPS4 in Arabidopsis. *Plant Cell, 24*(3), 1271-1284.

Mao, G., Meng, X., Liu, Y., Zheng, Z., Chen, Z., & Zhang, S. (2011). Phosphorylation of a WRKY transcription factor by two pathogen-responsive MAPKs drives phytoalexin biosynthesis in Arabidopsis. *Plant Cell, 23*(4), 1639-1653.

March-Diaz, R., Garcia-Dominguez, M., Lozano-Juste, J., Leon, J., Florencio, F. J., & Reyes, J. C. (2008). Histone H2A.Z and homologues of components of the SWR1 complex are required to control immunity in Arabidopsis. *Plant J, 53*(3), 475-487.

Martin, G., Brommonschenkel, S., Chunwongse, J., Frary, A., Ganal, M., Spivey, R., . . . Tanksley, S. (1993). Map-based cloning of a protein kinase gene conferring disease resistance in tomato. *Science, 262*(5138), 1432-1436.

McNellis, T. W., Mudgett, M. B., Li, K., Aoyama, T., Horvath, D., Chua, N. H., & Staskawicz, B. J. (1998). Glucocorticoid-inducible expression of a bacterial avirulence gene in transgenic Arabidopsis induces hypersensitive cell death. *Plant J, 14*(2), 247-257.

Meinhart, A., Kamenski, T., Hoeppner, S., Baumli, S., & Cramer, P. (2005). A structural perspective of CTD function. *Genes Dev, 19*(12), 1401-1415.

Mindrinos, M., Katagiri, F., Yu, G.-L., & Ausubel, F. M. (1994). The A. thaliana disease resistance gene RPS2 encodes a protein containing a nucleotide-binding site and leucine-rich repeats. *Cell, 78*(6), 1089-1099.

Miya, A., Albert, P., Shinya, T., Desaki, Y., Ichimura, K., Shirasu, K., . . . Shibuya, N. (2007). CERK1, a LysM receptor kinase, is essential for chitin elicitor signaling in Arabidopsis. *Proc. Natl Acad. Sci. USA, 104*(49), 19613-19618.

Monaghan, J., & Zipfel, C. (2012). Plant pattern recognition receptor complexes at the plasma membrane. *Curr Opin Plant Biol, 15*(4), 349-357.

Mosley, A. L., Pattenden, S. G., Carey, M., Venkatesh, S., Gilmore, J. M., Florens, L., . . . Washburn, M. P. (2009). Rtr1 is a CTD phosphatase that regulates RNA polymerase II during the transition from serine 5 to serine 2 phosphorylation. *Mol Cell, 34*(2), 168-178.

Murdock, C. C., Paaijmans, K. P., Cox-Foster, D., Read, A. F., & Thomas, M. B. (2012). Rethinking vector immunology: the role of environmental temperature in shaping resistance. *Nat Rev Microbiol, 10*(12), 869-876.

Nakagami, H., Soukupová, H., Schikora, A., Zárský, V., & Hirt, H. (2006). A mitogen-activated protein kinase kinase kinase mediates reactive oxygen species homeostasis in Arabidopsis. *Journal of Biological Chemistry, 281*(50), 38697-38704.

Nürnberger, T., Brunner, F., Kemmerling, B., & Piater, L. (2004). Innate immunity in plants and animals: striking similarities and obvious differences. *Immunological Reviews, 198*(1), 249-266.

Phatnani, H. P., & Greenleaf, A. L. (2006). Phosphorylation and functions of the RNA polymerase II CTD. *Genes Dev, 20*(21), 2922-2936.

Poltorak, A., He, X. L., Smirnova, I., Liu, M. Y., Van Huffel, C., Du, X., . . . Beutler, B. (1998). Defective LPS signaling in C3H/HeJ and C57BL/10ScCr mice: Mutations in Tlr4 gene. *Science, 282*(5396), 2085-2088.

Qiu, H., Hu, C., & Hinnebusch, A. G. (2009). Phosphorylation of the Pol II CTD by KIN28 enhances BUR1/BUR2 recruitment and Ser2 CTD phosphorylation near promoters. *Mol Cell, 33*(6), 752-762.

Ranf, S., Eschen-Lippold, L., Pecher, P., Lee, J., & Scheel, D. (2011). Interplay between calcium signalling and early signalling elements during defence responses to microbe-or damage-associated molecular patterns. *Plant J, 68*(1), 100-113.

Roux, M., Schwessinger, B., Albrecht, C., Chinchilla, D., Jones, A., Holton, N., . . . Zipfel, C. (2011). The Arabidopsis leucine-rich repeat receptor–like kinases BAK1/SERK3 and BKK1/SERK4 are required for innate immunity to hemibiotrophic and biotrophic pathogens. *Plant Cell, 23*(6), 2440-2455.

Samach, A., & Wigge, P. A. (2005). Ambient temperature perception in plants. *Curr Opin Plant Biol, 8*(5), 483-486.

Sim, R. J., Belotserkovskaya, R., & Reinberg, D. (2004). Elongation by RNA polymerase II: the short and long of it. *Genes & development, 18*(20), 2437-2468.

Smirnova, A., Li, H., Weingart, H., Aufhammer, S., Burse, A., Finis, K., . . . Ullrich, M. S. (2001). Thermoregulated expression of virulence factors in plant-associated bacteria. *Arch Microbiol, 176*(6), 393-399.

Song, W. Y., Wang, G. L., Chen, L. L., Kim, H. S., Pi, L. Y., Holsten, T., . . . Ronald, P. (1995). A receptor kinase-like protein encoded by the rice disease resistance gene, Xa21. *Science, 270*(5243), 1804-1806.

Spoel, S. H., & Dong, X. (2012). How do plants achieve immunity? Defence without specialized immune cells. *Nat Rev Immunol, 12*(2), 89-100.

Staskawicz, B. J., Dahlbeck, D., & Keen, N. T. (1984). Cloned avirulence gene of Pseudomonas syringae pv. glycinea determines race-specific incompatibility on Glycine max (L.) Merr. *Proc. Natl Acad. Sci. USA, 81*(19), 6024-6028.

Stuart, L. M., Paquette, N., & Boyer, L. (2013). Effector-triggered versus pattern-triggered immunity: how animals sense pathogens. *Nature Reviews Immunology*, 13(3): 199-206.

Suarez-Rodriguez, M. C., Adams-Phillips, L., Liu, Y., Wang, H., Su, S.-H., Jester, P. J., . . . Krysan, P. J. (2007). MEKK1 is required for flg22-induced MPK4 activation in Arabidopsis plants. *Plant physiology, 143*(2), 661-669.

Ueda, A., Li, P., Feng, Y., Vikram, M., Kim, S., Kang, C. H., . . . Koiwa, H. (2008). The Arabidopsis thaliana carboxyl-terminal domain phosphatase-like 2 regulates plant growth, stress and auxin responses. *Plant Mol Biol, 67*(6), 683-697.

Ullrich, M., Penaloza-Vazquez, A., Bailey, A. M., & Bender, C. L. (1995). A modified two-component regulatory system is involved in temperature-dependent biosynthesis of the Pseudomonas syringae phytotoxin coronatine. *J Bacteriol, 177*(21), 6160-6169.

Untergasser, A., Cutcutache, I., Koressaar, T., Ye, J., Faircloth, B. C., Remm, M., & Rozen, S. G. (2012). Primer3—new capabilities and interfaces. *Nucleic acids research, 40*(15), e115-e115.

van Dijk, K., Fouts, D. E., Rehm, A. H., Hill, A. R., Collmer, A., & Alfano, J. R. (1999). The Avr (effector) proteins HrmA (HopPsyA) and AvrPto are secreted in culture from Pseudomonas syringae pathovars via the Hrp (type III) protein secretion system in a temperature- and pH-sensitive manner. *J Bacteriol, 181*(16), 4790-4797.

Veronese, P., Nakagami, H., Bluhm, B., Abuqamar, S., Chen, X., Salmeron, J., . . . Mengiste, T. (2006). The membrane-anchored BOTRYTIS-INDUCED KINASE1 plays distinct roles in Arabidopsis resistance to necrotrophic and biotrophic pathogens. *Plant cell, 18*(1), 257-273.

Wang, W., Barnaby, J. Y., Tada, Y., Li, H., Tor, M., Caldelari, D., . . . Dong, X. (2011). Timing of plant immune responses by a central circadian regulator. *Nature, 470*(7332), 110-114.

Wang, Y., Bao, Z., Zhu, Y., & Hua, J. (2009). Analysis of temperature modulation of plant defense against biotrophic microbes. *Mol Plant Microbe Interact, 22*(5), 498-506.

Wang, Z.-Y. (2012). Brassinosteroids modulate plant immunity at multiple levels. *Proc. Natl Acad. Sci. USA, 109*(1), 7-8.

Wei, Z. M., Sneath, B. J., & Beer, S. V. (1992). Expression of Erwinia amylovora hrp genes in response to environmental stimuli. *J Bacteriol, 174*(6), 1875-1882.

Whitham, S., Dinesh-Kumar, S. P., Choi, D., Hehl, R., Corr, C., & Baker, B. (1994). The product of the tobacco mosaic virus resistance gene N: similarity to toll and the interleukin-1 receptor. *Cell, 78*(6), 1101-1115.

Yang, S., & Hua, J. (2004). A haplotype-specific Resistance gene regulated by BONZAI1 mediates temperature-dependent growth control in Arabidopsis. *Plant Cell, 16*(4), 1060-1071.

Young, R. A. (1991). RNA polymerase II. *Annu Rev Biochem, 60*, 689-715.

Zhang, J., Li, W., Xiang, T., Liu, Z., Laluk, K., Ding, X., . . . Zhou, J. M. (2010). Receptor-like cytoplasmic kinases integrate signaling from multiple plant immune receptors and are targeted by a Pseudomonas syringae effector. *Cell Host Microbe, 7*(4), 290-301.

Zhu, Y., Qian, W., & Hua, J. (2010). Temperature modulates plant defense responses through NB-LRR proteins. *PLoS Pathog, 6*(4), e1000844.

Zipfel, C., Kunze, G., Chinchilla, D., Caniard, A., Jones, J. D., Boller, T., & Felix, G. (2006). Perception of the bacterial PAMP EF-Tu by the receptor EFR restricts Agrobacterium-mediated transformation. *Cell, 125*(4), 749-760.

Zipfel, C., Robatzek, S., Navarro, L., Oakeley, E. J., Jones, J. D., Felix, G., & Boller, T. (2004). Bacterial disease resistance in Arabidopsis through flagellin perception. *Nature, 428*(6984), 764-767.